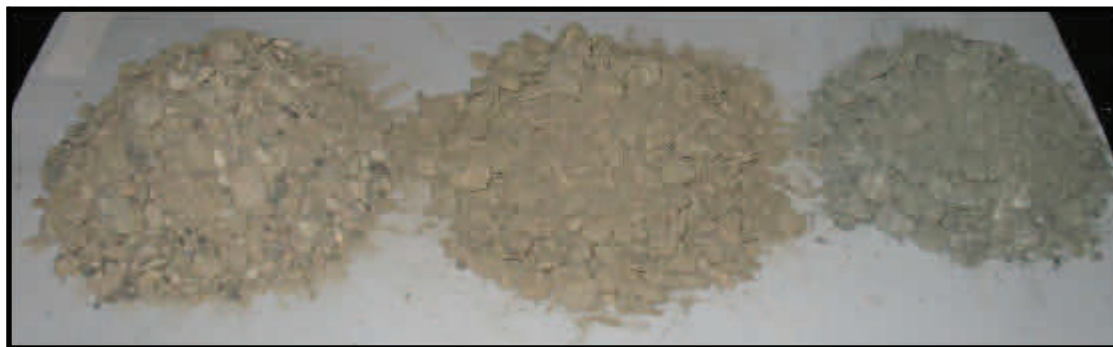# Characterization of Asphalt Treated Base Course Material

Final Report

Prepared By:
Peng Li
Juanyu Liu, Ph.D., P.E.

June 2010

Prepared By:

Alaska University Transportation Center
Duckering Building Room 245
P.O. Box 755900
Fairbanks, AK 99775-5900

Alaska Department of Transportation
Research, Development, and Technology
Transfer
2301 Peger Road
Fairbanks, AK 99709-5399

INE/ AUTC #11.02

DOT # FHWA-AK-RD-10-07

REPORT DOCUMENTATION PAGE

Form approved OMB No.

1. AGENCY USE ONLY (LEAVE BLANK)	2. REPORT DATE	3. REPORT TYPE AND DATES COVERED
FHWA-AK-RD-10-07	June 2010	Final Report (8/2007-8/2009)

4. TITLE AND SUBTITLE
Characterization of Asphalt Treated Base Course Material

5. FUNDING NUMBERS
AUTC#107049
DTRT06-G-0011
T2-06-09

6. AUTHOR(S)
Juanyu Liu
Peng Li

7. PERFORMING ORGANIZATION NAME(S) AND ADDRESS(ES)
Alaska University Transportation Center
P.O. Box 755900
Fairbanks, AK 99775-5900

8. PERFORMING ORGANIZATION REPORT NUMBER

INE/AUTC # 11.02

9. SPONSORING/MONITORING AGENCY NAME(S) AND ADDRESS(ES)
Alaska Department of Transportation
Research, Development, and Technology Transfer
2301 Peger Road
Fairbanks, AK 99709-5399

10. SPONSORING/MONITORING AGENCY REPORT NUMBER

FHWA-AK-RD-10-07

11. SUPPLENMENTARY NOTES

12a. DISTRIBUTION / AVAILABILITY STATEMENT

No restrictions

12b. DISTRIBUTION CODE

13. ABSTRACT (Maximum 200 words)

Asphalt-treated bases are often used in new pavements; the materials are available and low-cost, but there is little data on how these materials perform in cold regions. This study investigated four ATB types (hot asphalt, emulsion, foamed asphalt, and reclaimed asphalt pavement) popular for treating base course materials. The research team collected data on stiffness, fatigue, and permanent deformation characteristics under different temperatures. This study produced a detailed literature review, including information from ongoing research projects, to compile the latest information concerning ATB characterization. Also completed were resilient modulus tests of ATB material commonly used for Alaska's northern and central regions, as well as rutting tests using a Georgia Loaded Wheel Test apparatus. Researchers conducted resilient modulus tests on specimens of foamed asphalt-treated base material, fabricated in ADOT&PF labs, in all three Alaska regions; an additional test was performed in the central region using different binder contents and soaked conditions. Statistical analysis of the effects of aggregate properties on the resilient modulus were completed and incorporated into the finalized model. Study recommendations noted that based on the predicting equations for resilient modulus (MR), the moduli of treated base course materials can be calculated according to treatment technique, ambient temperature, aggregate properties, and binder content.

14- KEYWORDS: Asphalt pavements (Pmrcppbmb), Asphalt (Rbeusb), Asphalt based materials (Rbmdpb), Asphalt emulsions (Rbmdyheb), Reclaimed asphalt pavements (Pmrcppbc), Foamed asphalt (Rbmdpbh), Modulus of resilience (Rkmyr)

15. NUMBER OF PAGES

16. PRICE CODE

N/A

17. SECURITY CLASSIFICATION OF REPORT	18. SECURITY CLASSIFICATION OF THIS PAGE	19. SECURITY CLASSIFICATION OF ABSTRACT	20. LIMITATION OF ABSTRACT
Unclassified	Unclassified	Unclassified	N/A

NSN 7540-01-280-5500

STANDARD FORM 298 (Rev. 2-98)
Prescribed by ANSI Std. 239-18 298-1

SI* (MODERN METRIC) CONVERSION FACTORS

APPROXIMATE CONVERSIONS TO SI UNITS

Symbol	When You Know	Multiply By	To Find	Symbol
LENGTH				
in	inches	25.4	millimeters	mm
ft	feet	0.305	meters	m
yd	yards	0.914	meters	m
mi	miles	1.61	kilometers	km
AREA				
in^2	square inches	645.2	square millimeters	mm^2
ft^2	square feet	0.093	square meters	m^2
yd^2	square yard	0.836	square meters	m^2
ac	acres	0.405	hectares	ha
mi^2	square miles	2.59	square kilometers	km^2
VOLUME				
fl oz	fluid ounces	29.57	milliliters	mL
gal	gallons	3.785	liters	L
ft^3	cubic feet	0.028	cubic meters	m^3
yd^3	cubic yards	0.765	cubic meters	m^3
NOTE: volumes greater than 1000 L shall be shown in m^3				
MASS				
oz	ounces	28.35	grams	g
lb	pounds	0.454	kilograms	kg
T	short tons (2000 lb)	0.907	megagrams (or "metric ton")	Mg (or "t")
TEMPERATURE (exact degrees)				
°F	Fahrenheit	5 (F-32)/9 or (F-32)/1.8	Celsius	°C
ILLUMINATION				
fc	foot-candles	10.76	lux	lx
fl	foot-Lamberts	3.426	candela/m^2	cd/m^2
FORCE and PRESSURE or STRESS				
lbf	poundforce	4.45	newtons	N
lbf/in^2	poundforce per square inch	6.89	kilopascals	kPa

APPROXIMATE CONVERSIONS FROM SI UNITS

Symbol	When You Know	Multiply By	To Find	Symbol
LENGTH				
mm	millimeters	0.039	inches	in
m	meters	3.28	feet	ft
m	meters	1.09	yards	yd
km	kilometers	0.621	miles	mi
AREA				
mm^2	square millimeters	0.0016	square inches	in^2
m^2	square meters	10.764	square feet	ft^2
m^2	square meters	1.195	square yards	yd^2
ha	hectares	2.47	acres	ac
km^2	square kilometers	0.386	square miles	mi^2
VOLUME				
mL	milliliters	0.034	fluid ounces	fl oz
L	liters	0.264	gallons	gal
m^3	cubic meters	35.314	cubic feet	ft^3
m^3	cubic meters	1.307	cubic yards	yd^3
MASS				
g	grams	0.035	ounces	oz
kg	kilograms	2.202	pounds	lb
Mg (or "t")	megagrams (or "metric ton")	1.103	short tons (2000 lb)	T
TEMPERATURE (exact degrees)				
°C	Celsius	1.8C+32	Fahrenheit	°F
ILLUMINATION				
lx	lux	0.0929	foot-candles	fc
cd/m^2	candela/m^2	0.2919	foot-Lamberts	fl
FORCE and PRESSURE or STRESS				
N	newtons	0.225	poundforce	lbf
kPa	kilopascals	0.145	poundforce per square inch	lbf/in^2

*SI is the symbol for the International System of Units. Appropriate rounding should be made to comply with Section 4 of ASTM E380.
(Revised March 2003)

ACKNOWLEDGMENT

EXECUTIVE SUMMARY

In many areas of Alaska, clean, durable aggregates normally utilized for base course either require long hauls from outside, or they are difficult to obtain within the project limits. The capacity to stabilize the available lower quality materials for use as base course strengthens pavements, thus extending their lifespans and saving the state money in the long run. Asphalt treated bases (ATBs) are the most commonly used type of stabilized layers in Alaska because of material availability and relative cost. At present there is a lack of data on engineering characteristics (properties) for typical Alaskan base materials, especially for the modulus of the stabilized base course, which is an essential parameter for material evaluation and pavement design. Recently this need has been made more critical by AKDOT&PF's adoption of mechanistic pavement design methods.

This study systematically investigated the engineering properties of three types of ATBs and mixture of reclaimed asphalt pavement (RAP) and granular base course material (D-1) at 50% to 50% ratio. D-1 materials were collected from three regions of Alaska: Southeast region, Central region, and Northern region, to investigate the effect of aggregate source on the properties of base course materials. Aggregate properties, such as fractured surface, were measured. Three types of treatment techniques were used, hot asphalt treated base (HATB), emulsified asphalt treated base (EATB) and foamed asphalt treated base (FATB). PG 58-28 binder was used for HATB and three binder contents were used, 2.5%, 3.5% and 4.5%. CSS-1 emulsion was used for EATB with three residual binder contents, 1.5%, 2.5% and 3.5%. PG 58-28 binder was also used to produce foamed asphalt. The residual binder contents applied for FATB was 1.5%, 2.5% and 3.5%. Cylindrical specimens were manufactured for ATBs and 50%:50% RAP and Resilient modulus (M_R) tests were performed on these specimens according to AASHTO-307. Tests were conducted at three temperatures, -10°C, $0\,^{o}$C and $20\,^{o}$C, which represented typical temperature at different seasons. Rutting tests were carried out for HATB. Beam fatigue tests were performed for HATB as well, but only for specimens with 3.5% and 4.5% binder contents.

The M_R testing results showed that asphalt treatment effectively increases moduli of D-1 material. Among three treatment techniques, hot asphalt treatment has the most significant improvement, followed by emulsified asphalt treatment and foamed asphalt treatment. In this study, no obvious improvement on the M_R has been observed on 50%:50% RPA specimens. All treated base course materials exhibited stress-state dependent properties. Generally, the M_Rs increased with the increase of confining pressure (σ_3) and deviatoric stress (σ_d). This dependency varies for different types of material. As expected, the M_Rs of ATBs increased with a decrease in temperature. It was also found that higher binder content for treatment did not increase the M_R of ATBs. Generally, low binder content produced higher moduli. However, this doesn't mean that ATBs with lower binder content have better performance when paved on the roadways. Aggregate source affects the M_R of ATBs as well. Northern region ATBs had the lowest M_R among three regions of Alaska due to least-angular D-1 material. Though statistical approach, predicting equations for M_R were developed for all treated based course materials based on the current stress-dependent AASHTO MEPDG model.

The rutting test results showed that HATB with 3.5% binder content has the best rutting resistance. Based on the beam fatigue test, HATB composed of southeast D-1 has the best rut resistance and the Northern HATB has the lowest. Increase the binder content greatly increased the fatigue resistance of HATB based on the test results on specimens with 3.5% and 4.5% binder content.

The M_R equations developed in this study are suggested to be further validated by conducting case studies of pavement designs using AKFPD and MEPDG design programs, and based on the recommended M_R and equations obtained from this study as material inputs.

TABLE OF CONTENTS

LIST OF FIGURES

LIST OF TABLES

CHAPTER I

INTRODUCTION

Engineers use stabilization to enhance materials properties for pavement design procedures or to overcome deficiencies in available materials. In many areas of Alaska, clean, durable aggregates normally utilized for base course either require long hauls from outside, or they are difficult to obtain within the project limits. Asphalt treated base (ATB) material is the most commonly used type of stabilized layers because of material availability and relative low cost in Alaska.

In this study, a comprehensive study was carried out to characterize three typical Alaska ATBs (i.e. hot asphalt treated base (HATB), emulsified asphalt treated base (EATB) and foamed asphalt treated base (FATB)), and reclaimed asphalt pavement (RAP) treated base materials. The effects of stress state, aggregate properties, asphalt content, and temperature on resilient modulus (M_R) of these materials were evaluated experimentally and design equations were developed. Resistances to fatigue and rutting of HATB materials were investigated as well.

PROBLEM STATEMENT

The Alaska Flexible Pavement Design (AKFPD) Manual and the statewide policy on base course stabilization stipulate the use of bound stabilized bases on all roadway construction, reconstruction and rehabilitation projects. The inclusion of asphalt (either hot or in the form of emulsion, and foam) is one of the options mentioned to construct ATBs.

The AKFPD method, which is a mechanistic-based design method, has been used widely in Alaska for pavement design and analysis (McHattie 2004). Material properties, such as M_R and Poisson's ratio at different seasons, are required inputs for the base course layer in the design procedure. The current default M_R values were obtained from back-calculated layer moduli after nondestructive field testing performed

by the Alaska Department of Transportation and Public Facilities (AKDOT&PF). On the other hand, the current American Association of State Highway and Transportation Officials (AASHTO) mechanistic empirical pavement design guide (MEPDG) offers predictive models for base course materials (ARA, Inc. 2000). However, these models cannot be confidently applied to Alaskan materials because of peculiar Alaskan conditions in terms of material properties and climatic (seasonal) differences. As M_R values of ATBs are influenced by various materials and climatic factors, there is a need to measure and characterize the engineering characteristics of typical Alaskan ATB materials for updating the database of material properties to be used in the current AKFPD and MEPDG.

OBJECTIVE

In this study, the following objectives are addressed:

- Systematically evaluating the stiffness, fatigue and permanent deformation characteristics of Alaskan ATB course materials,
- Investigating the effects of different stabilization levels (i.e. residual asphalt content) and environmental conditions (i.e. temperature) on the performance of Alaskan ATB course materials,
- Developing M_R equations to be incorporated in the AKFPD and MEPDG programs, and
- Providing recommendations for use of ATBs for designers in their new design projects.

RESEARCH METHODOLOGY

To meet the objectives of this study, the following major tasks were accomplished:

- Task 1:   Literature Survey
- Task 2:   Laboratory Investigation

- Task 3:   Data Processing and Analyses

- Task 4:   Conclusions and Recommendations

Task 1: Literature Survey

This task involved a comprehensive literature search of published materials and on-going research projects to obtain the latest information related to ATB characterization. The characterization of ATBs included evaluation of material properties such as M_R, permanent deformation, rutting resistance and fatigue resistance. Historical concept development, testing methods, influencing factors and modeling of material properties were briefly presented as well. This task is documented in chapter II.

Task 2: Laboratory Investigation

For each type of ATB course, three D-1 base course materials commonly used in three regions of the Alaska state were selected. The aggregate properties were evaluated prior to the mix design, and those properties included aggregate gradation, moisture content, abrasion resistance, percentage of fractured face, and flat or elongated particles. The asphalt binder used for HATB in this study was PG 52-28 asphalt. The emulsified asphalt used for EATB was CSS-1, a cationic emulsion with low viscosity. The foamed asphalt was generated by using PG 52-28 asphalt with a foamed asphalt lab unit (WLB10). Three binder contents were used to stabilize each kind of ATB (HATB: 2.5%, 3.5% and 4.5%; EATB and FATB: 1.5%, 2.5%, and 3.5%). A 50:50 mixture of RAP and D-1 granular material was also selected as a treated base.

Engineering properties of ATB course materials were evaluated including M_R, permanent deformation, fatigue life, and rutting performance. The triaxial test was utilized to evaluate the M_R and permanent deformation of ATBs. The tests were conducted according to AASHTO T307 at various stress states. To investigate the effects of influencing factors such as temperature, binder content and aggregate

source, tests were performed in a temperature control chamber at three temperatures. The effect of aggregate source was also investigated by performing tests on specimens with D-1 materials from three regions in Alaska.

Rutting and fatigue tests were performed using Georgia loader wheel tester (GLWT) and repeated flexural bending system, separately. The tests were only conducted on HATB. For GLWT, specimens prepared with D-1 from three regions at three binder contents were tested. Fatigue tests were performed under strain controlled loading pattern at three loading levels for three regions. Fatigue tests were only performance on specimens with two binder contents, 3.5% and 4.5%. The detailed experimental design is presented in Chapter III.

Task 3: Data Processing and Analyses

Testing data obtained from previous task were analyzed in this task. Statistical methods were used to analyze M_R data of three types of ATBs. Comprehensive regression models were then developed to reflect the effects of stress states, temperature, binder content and aggregate source on performance of ATBs. Data from rutting tests of HATBs were illustrated to indicate the development of the rutting depth during the repeated loading process. Influencing factors including binder content and aggregate source were evaluated. Regression analysis was performed based on the data from fatigue tests of HATBs, and the effect of binder content was also investigated. The detailed data analysis and testing results are elaborated in Chapter IV and appendix.

Task 4: Conclusions and Recommendations

Based upon the above tasks, a summary of research results and findings from this study was provided in this task. Recommendations regarding use of ATBs for Alaska pavement design and construction were made, as well as those for future work, as presented in Chapter V.

CHAPTER II

LITERATURE REVIEW

This chapter presents a comprehensive review of previous studies related to characterizing asphalt treated base course materials. The review includes introduction of ATBs, resilient modulus (M_R) of base course materials, fatigue performance and rutting resistance. For each material property, such as M_R, testing methods, influencing factors and models were summarized.

INTRODUCTION OF ASPHALT TREATED BASE COURSE

Compare to untreated granular base, ATBs increase the stiffness of base course layer, leading to more efficient load distribution. It also improves durability and reduces the frost heave susceptibility. Depending on the type of treatment applied to a granular material, there are three types of ATBs used in Alaska: hot asphalt treated base (HATB), emulsified asphalt treated base (EATB), and foamed-asphalt treated base (FATB).

Hot asphalt treated base (HATB) is a dense-graded hot mix asphalt (HMA) with a wide gradation band and lower asphalt content. Usually, granular material used for HATB has a lower quality than HMA. Therefore, the cost of HATB is less. Emulsified asphalt treated base (EATB) is a cold mixture of emulsified asphalt and granular material. Emulsified asphalt is a mixture of asphalt and water assisted by an emulsifying agent. This technique greatly reduces the viscosity of asphalt at low temperature, which makes it possible to produce asphalt mixture at room temperature. Foamed-asphalt treated base (FATB) is also a cold treatment technique. As shown in Figure 2.1, the foamed asphalt is produced by injecting small amounts of water (approx. 2–3% by weight of asphalt) to hot asphalt (Wirtgen 2002). Due to the immediate water evaporation, asphalt expands 15 to 20 times of its original volume, leading to great viscosity reduction of asphalt. FATB can be produced both in plant and in-site.
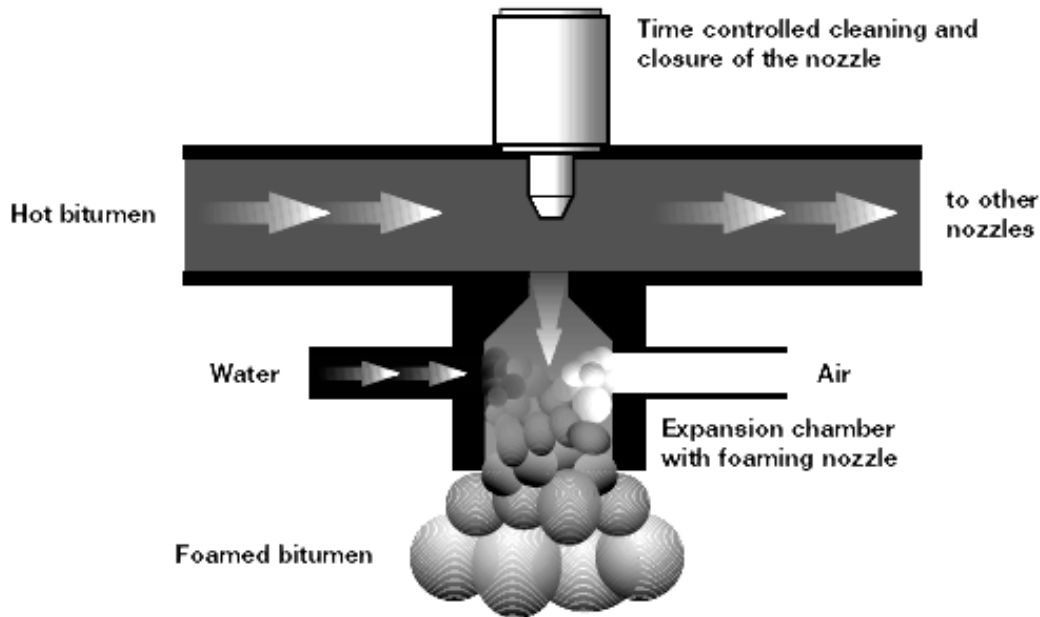
Figure 2.1 Production Process of Foamed Asphalt

M_R OF BASE COURSE MATERIALS

In elastic theory, the elastic modulus, which represents the stress-strain relationship of a material, is one of the fundamental parameters used for mechanistic analysis. However, most materials used for highway construction are not pure elastic. To solve this problem, the concept of M_R has been developed by simplifying the real condition. If the load is relatively small compared to the strength of the material, the permanent deformation is negligible and the material can be considered elastic. On the other hand, the pavement is subject to repeated traffic load. Research showed that there was a considerable difference between tangent modulus determined from static loading and determined from repeated loading (Figure 2.2). It indicates that the behavior of pavement material under traffic loading can be only obtained from repeated loading tests (Seed et al. 1955, Seed and Mcneill 1958, Seed et al. 1963). Therefore, M_R is defined as maximum repeated load divided by recoverable strain (Huang, 2004):

$$M_R = \frac{\sigma_d}{\varepsilon_r} \qquad\qquad (2.1)$$

where σ_d is the deviator stress, which is the axial stress in an unconfined compression test or the axial stress in excess of the confining pressure, expressed as σ_1-σ_3, in a triaxial compression test and ε_r is the recoverable strain under repeated loads.
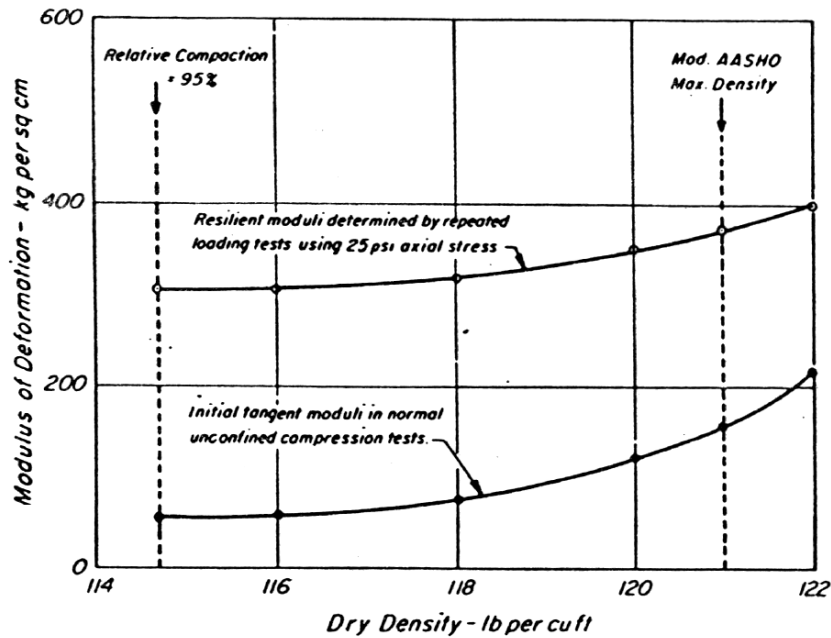
Figure 2.2 Comparison of Modului of Deformation Determined by Normal Unconfined Compression and Repeated Loading Tests (Seed and McNeill 1958)

Determination of M_R

In the past, the M_R of pavement material has been determined through three approaches: (1) measuring M_R by laboratory testing, (2) through field test, such as repeated plate load and falling weight deflectometer (FWD) tests, and (3) predicting the M_R using physical and mechanical properties of the material based on available correlations.

Laboratory testing

In the laboratory test, the M_R of pavement material is determined through repeated loading. Researchers have investigated which kinds of loading pattern could represent the real traffic load (Barksdale 1971, Brown 1973, Terrel et al. 1974). The results showed that vehicle speed, depth beneath the pavement surface and rest period between individual pulses were of great importance in selecting the appropriate loading pattern. The load pattern of 0.1s haversine pulse combined with 0.9s rest period has been wildly accepted as the standard loading form for M_R test.

Most commonly, there are two tests used to determine the M_R of pavement materials:

- Indirect tensile test (IDT)

- Triaxial compression test

The indirect tensile test was developed independently in Brazil and Japan around same time (Kennedy and Hudson 1968). Biscuit shape specimen is used for this test. During the testing, the load is applied vertically through the diametral path of the specimen and maximum tensile stress is developed along vertical diameter, as show in Figure 2.3. The calculation of M_R is based on the theoretical equations listed below according to ASTM D4123 (1995):

$$E_{RI}=P(v_{RI}+0.27)/t\Delta H_I \qquad\qquad (2.2)$$

$$E_{RT}=P(v_{RT}+0.27)/t\Delta H_T \qquad\qquad (2.3)$$

$$v_{RI}=3.59\Delta H_I/\Delta V_I -0.27 \qquad\qquad (2.4)$$

$$v_{RI}=3.95\Delta H_T/\Delta V_T-0.27 \qquad\qquad (2.5)$$

where,

E_{RI} = instantaneous resilient modlulus of elasticity, psi (or MPa),

E_{RT} = total resilient modlulus of elasticity, psi (or MPa),

v_{RI} = instantaneous resilient Poisson's ration,

v_{RI} = total resilient Poisson's ration,

P = repeated load, lbf (or N),

t   = thickness of specimen, in. (or mm),

ΔH_I = instantaneous recoverable horizontal deformation, in. (or mm),

ΔV_I = instantaneous recoverable vertical deformation, in. (or mm),

ΔH_T = total recoverable horizontal deformation, in. (or mm), and

ΔV_T = total recoverable vertical deformation, in. (or mm).

a)   b)
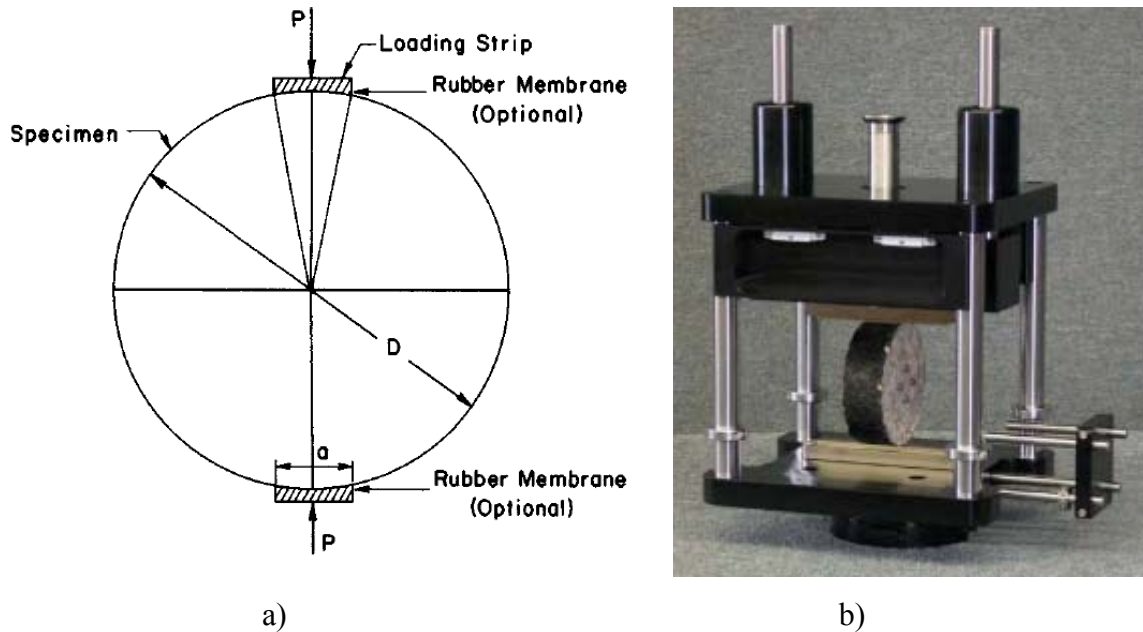
Figure 2.3 Indirect Tensile Test

The advantages of this test are: (1) the test is relatively simple and easy to perform, (2) specimens are easy to fabricate and the thin field cores can be used for testing, (3) the test can provide information of tensile strength, Poisson's ratio and permanent deformation of the materials, and (4) the variation of test results is low compared to triaxial test. However, this method is not capable to control the stress state in three dimensions to investigate the stress dependent properties of pavement materials (Barksdal et al. 1997, Fu and Harvey 2007). In addition, because there isn't confining pressure applied during the test, loose materials can not be tested by this method. Generally, indirect tensile test is preferred for heavily bounded material, such as asphalt concrete.

In the triaxial test, the testing system applies both a vertical load and a confining pressure on cylindrical specimens, as shown in Figure 2.4. As a result, the stress condition within the specimen is well

controlled. The stress state is relatively simple and straightforward compared to the indirect tensile test. The calculation of M_R follows Equation 2.1. All kinds of materials can be tested using this method. The main disadvantages of this testing method are its cost and the relative complexity of the necessary testing equipment. In addition, if the sample is composed of coarse aggregates, it requires a large size sample to perform M_R tests. Field samples directly cored from thin pavement layers could not be tested by this method. These disadvantages embarrass the triaxial test to become a daily routine test method.

Note: $\Theta = \sigma_1 + \sigma_2 + \sigma_3 = \sigma_d + 3\sigma_3$
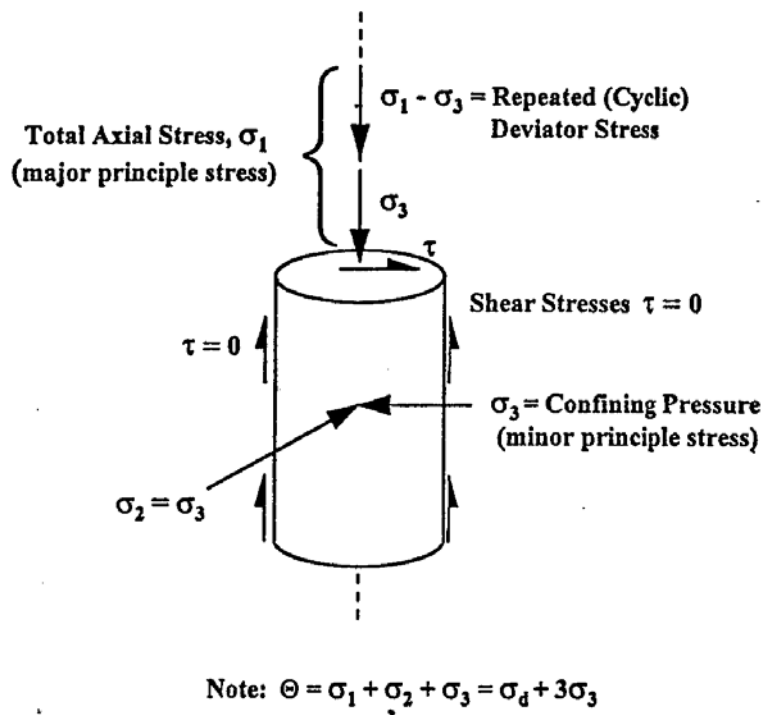
Figure 2.4 Triaxial Test

Field testing

Repeated plate load test is one of the oldest testing methods used to investigate the deformation and resilient behavior of subgrade soil (Figure 2.5). The early work on this subject has been done during 1940s (Mcleod 1947, Hittle and Goetz 1947). Repeated plate load test is costly and time consuming.

A FWD test is a field none-destructive testing that simulates deflection of a pavement surface caused by a fast-moving truck. During the test, the FWD generates a load pulse by dropping a weight and then this load pulse is transmitted to the pavement. The analysis of testing results provides the effective roadway M_R, the effective in-situ structural number, the pavement layer moduli, the effective in-situ layer coefficient (Gartin and Esch 1991, Zaghloul et al., 1998, Hossain et al., 2000, Noureldin et al., 2004;). However, the back-calculation procedure is based on a combination of Boussinesq and elastic theories and assumed Poisson's ratio. The back calculated values need to be adjusted based on the record of laboratory measured moduli (AASHTO 1993).
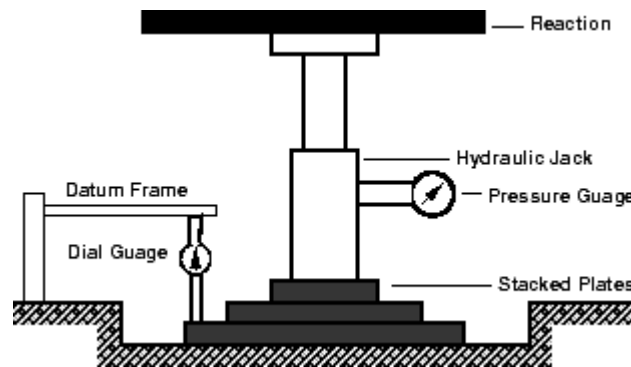
Figure 2.5 Repeated Plate Load Test

Predicting M_R from empirical correlation

Various empirical tests have been used to characterize the pavement material. Most of tests are simple to perform and wildly adopted as routine tests, such as Marshall stability test and California bearing ratio (CBR) test. The correlations between M_Rs and the testing results from these tests have been developed. The coefficients in these correlations vary according to local practices. For asphalt concrete, the most well known predicting method was proposed by Nijboer (1957) using Marshall stability-flow ratio as follows:

$$S_{60^o C, 4\sec} = 1.6(\text{stability/flow}) \tag{2.6}$$

where S is the modulus given in kilograms per square centimeter, stability in kilograms, and flow in millimeters. Later, this equation was modified by McLeod (1967) using English units:

$$M_R = 40(\text{stability/flow}) \tag{2.7}$$

where M_R is given in psi, stability in pounds and flow in inches.

Another empirical correlation used to predict M_R, which is typically used for fine-grained soils, was suggested by Heukelom and Klomp (1962) using CBR as show in Equation 2.8. For coarse-grained soils, Equation 2.9 was used (VDOT 2000)

$$M_R = 1500 \times CBR \tag{2.8}$$

$$M_R = 3000 \times CBR^{0.65} \tag{2.9}$$

where M_R is in the unit of psi.

Influencing factors

Several factors are considered significantly influencing the M_R of ATBs, including asphalt binder, temperature, air void content, stress state and aggregate properties.

Asphalt Binder

Asphalt binder is one of the most important influencing factors for M_R of ATBs. Binder performs as a glue holding all aggregate particles together and improving the stiffness and durability of base course materials. The stiffness of binder itself has a strong effect on the M_R of asphalt treated material. The M_R of asphalt treated material tends to increase with the increment of the high temperature grade of binder and associated stiffness (Pan et al. 2005). The fitting equations developed by Terrel and Awad (1972) showes that the M_R of HATB decreases with the increase of binder content. For FATB, there is an optimum binder content, at which the material reaches the highest M_R (Muthen 1998, Nataatmadja 2001, Kim and Lee 2006).

Temperature

Since asphalt cement is a thermoplastic material in nature (Roberts et al. 1996), its stiffness dramatically increases with the decrease of temperature. The M_R of ATBs also varies with the change of temperature. Terrel and Awad (1972) found that the M_R of HATB decreased sharply when temperature increased. However, as FATB is lightly bound by dispersed asphalt droplets, studies (Bissada 1987, Nataatmadja 2001, Fu and Harvey 2007) concluded that FATB was less sensitive to temperature than HATB.

Stress state

Previous studies, from early study done by Terrel and Awad (1972) to recent one by Fu and Harvey (2007), showed without exception that, the M_R of ATBs presented the stress dependent properties, to the extent which may wary according to types of materials. Terrel and Awad (1972) concluded that low asphalt contents did not provide adequate cementation of the aggregate particles particularly if high percentages of fines were used. Therefore, the behavior of these mixtures was close to the unbound aggregate with considerable dependency on confining pressures. It had also been mentioned that some asphalt mixes under special environments, such as saturated samples at high temperature, exhibited large permanent deformation but very little or even no resilient strain. In this case, if the concept of M_R is applied, it will result an extraordinarily high modulus. Instead, an additional modulus relating the stress and total strains should be used. The previous research done by Anderson and Thompson (1995) showed that M_R of EATB increased as the increase of bulk stress, which was the summation of three principle stresses. Later, through the laboratory testing, Fu and Harvey (2007) found that, this phenomenon also applied to FATB.

Air voids

Air void content is one of most important volumetric parameters for asphalt mixtures (Roberts 1996). It relates to almost every single aspect of asphalt mixture performance. As Terrel and Awad indicated in their study (1972), increase of air void led to decrease of modulus of HATB. In addition, recent reseach

13

(Shu and Huang, 2008) revealed that, not only air void content, but also the air void size distribution also palyed an important role in the modulus of asphalt mixtures. "Larger air bubbles entrapped in the mixture do more harm to the dynamic modulus than smaller bubbles."

Aggregate properties

Aggregate properties include gradation, particle shape, angularity, surface texture, abrasion resistance and etc. Gradation is the particle size distribution of certain kind of aggregate. As the ratio of fine to coarse aggregate increases, the M_R decreases (Hodek 2007). Shape and surface texture also have great influence on the performance of asphalt-treated materials (Kandhal and Parker 1998, Prowell et al. 2005), in which aggregates are relied upon to provide stiffness and strength by interlocking with another. Based on the image analyzing system, Pan et al. (2005) concluded that coarse aggregates with better angularity and surface texture significantly improved the M_R of asphalt mixtures.

Reclaimed asphalt pavement (RAP) is also treated as aggregate being reused for road reconstruction or rehabilitation. Previous study (Kim et al. 2007) showed that, generally, the base course material produced with RAP, the content of which varies from 25% to 75%, performed at a similar level to 100% virgin aggregate in terms of M_R and strength when properly compacted. However, it exhibited at least two times greater permanent deformation than 100% virgin aggregate material.

Modeling M_R

In the past several decades, considerable effort has been spent in modeling the behavior of ATBs. The K−θ model (Hicks and Monismith 1971, Kalcheff and Hicks 1973) is the most popular model to address the stress dependent properties of base course materials (Equation 2.10). A linear relationship between M_R and bulk stress can be easily observed by plotting the testing results in log-log scale. The disadvantage of K−θ model is that the important effect of shear stress is not considered (May and Witczak 1981). Later, Uzan (1985) developed a model (Equation 2.11) that overcame this deficiency by adding the deviator

stress (σ_d) into the K$-\theta$ model. Deviator stress is directly related to the maximum shear stress applied to the specimen during testing.

As shown in Equation 2.12, considering that the triaxial test is a three-dimensional test, σ_d is replaced by the octahedral stress (τ_{oct}) (Witczak and Uzan 1988). In the recent AASHTO mechanistic empirical pavement design guide (MEPDG) (ARA, Inc. 2000), the model is further modified from the octahedral stress model by adding atmosphere pressure (Equation 2.13). The advantage of adding atmosphere pressure is that the same regression constants in this model can be used in both English units system and metric system. The effects of material components and testing conditions have been also introduced into the model by correlating these factors with the regression constants (Santha 1994).

$$M_R = k_1 \theta^{k_2} \tag{2.10}$$

$$M_R = k_1 \theta^{k_2} \sigma_d^{k_3} \tag{2.11}$$

$$M_R = k_1 \theta^{k_2} \tau_{oct}^{k_3} \tag{2.12}$$

$$M_R = k_1 P_a \left(\frac{\theta}{P_a}\right)^{k_2} \left(\frac{\tau_{oct}}{P_a} + 1\right)^{k_3} \tag{2.13}$$

where,

M_R = resilient modulus, ksi,

θ = bulk stress, $\sigma_1 + \sigma_2 + \sigma_3$, psi,

σ_d = deviator stress, psi,

τ_{oct} = deviator stress, $1/3[(\sigma_1-\sigma_2)^2+(\sigma_1-\sigma_3)^2+(\sigma_2-\sigma_3)^2]^{1/2}$, psi,

P_a = atmosphere air pressure, psi, and

k_1, k_2, k_3 = regression constants.

FATIGUE PERFORMANCE

Fatigue cracking is one of the primary distresses in flexible pavement (Huang 2004). The fatigue resistance of an asphalt mix is its ability to withstand repeated loading without fracture. It is important to characterize the fatigue performance of specific mixes over a range of loading and environmental conditions so that it can be incorporated into the process of flexible pavement design.

Testing methods

Generally, there are two methods wildly used to investigate the fatigue performance of asphalt mixture, flexural beam bending test and indirect tensile test. The advantages of these two test methods are: (1) the tests simulate field conditions, (2) the test results can be used for modeling pavement performance, (3) they are relatively easy to be performed and (4) the results correlate to the performance of in-service pavements.

Flexural Beam Bending Test

During the flexural beam bending test, an asphalt-concrete beam specimen is simply supported at each end and subjected to a repeated controlled load (stress) or deflection (strain) under either third-point (Figure 2.6) or center-point loading. One advantage of third-point loading is that a larger portion of the specimen is subjected to a uniform maximum stress level. Thus the likelihood is greater in beam testing that test results will reflect the weaknesses that naturally occur in the beam. The four-point bending method has been adopted by AASHTO T321. When to stop a flexural fatigue test depends on the test mode and purpose. For the constant stress mode, the test is continued until the beam actually breaks. For the constant strain mode, failure is more difficult to define because in order to keep the strain constant the applied stress is continually reduced, which results in a beam that never really breaks. Therefore, in constant strain mode, failure is normally defined as the point at which the load or stiffness reaches some predetermined

values; most typically 50 percent of the original value. The controlled-stress mode of loading appears to represent the response of thick asphalt pavements to repetitive loading while the controlled-strain approach is suitable for thin pavements.

The following are considered to be the primary advantages of simple flexure tests (Tangella et. al. 1990):

1. This test method is well known, widespread in use, and readily understood.

2. The basic technique measures a fundamental property that can be used for.

3. The results can be used directly (with an appropriate shift factor) in the structural design of pavements to estimate the propensity for cracking.

4. Results of controlled-stress testing can be used for the design of thick asphalt pavements whereas results of controlled-strain testing can be used for the design of thin asphalt pavements.
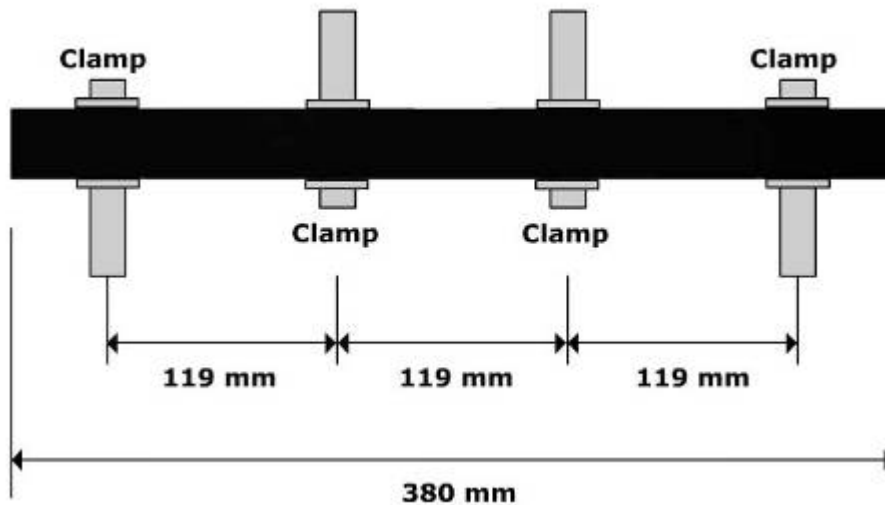
Figure 2.6 Sketch of Four Point Bending Beam Test

The major limitations of this methodology are:

1. Validation of laboratory results by comparison with in-situ pavement performance is difficult.

2. The method is costly, time consuming, and requires specialized equipment.

3. Unlike that within the pavement structure, the state of stress is essentially uniaxial.

4. Elastic theory is usually assumed to compute the tensile strain or stress.

Indirect Tensile Test

The test set up of indirect tensile fatigue test is similar as that used for M_R test (Figure 2.3). The advantages of this method are: (1) the thin cylindrical specimen used for testing is easy to be fabricated, (2) field cores can be used for testing, and (3) air void content in the asphalt mix can be controlled very well. However, only stress controlled model can be applied during the test. The reason that strain controlled mode can not be applied is that the mechanism of forcing the deformation (either horizontal or vertical) back to the original position is not available. The loading strip could be glued to the specimen in order to control the vertical strain. However, this mechanism will develop a plane of maximum tensile stress along the horizontal diameter when the loading head moves upward, which violates the theory behind the indirect tensile test. This method significantly underestimates fatigue life relative to other laboratory methods (Tangella et. al. 1990).

Influencing factors

The fatigue performance of asphalt mixture is primarily determined by its material variables such as air void content, binder content, type of binder and aggregate properties. On in-service roadways, the fatigue life of a certain asphalt mixture was determined by the repeated loads and environmental conditions.

Material Variables
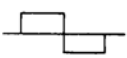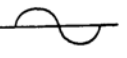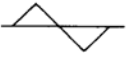
Air void and binder contents are the two primary material variables, which affects fatigue life of an asphalt mixture (Pell 1972, Pell 1973, Monismith et al. 1970, Epps et al. 1972). The air void should be as small as possible (but not less than the minimum limit of 3.0 percent) to obtain the greatest fatigue life and the asphalt content should be as high as possible with due consideration to stability. The optimum asphalt content to obtain a maximum fatigue life is generally higher than the design required for rutting considerations. The fatigue performance is also sensitive to the type of asphalt binder, which could be explained on the basis of its loss stiffness correlating to the fatigue life of mixtures (Deacon, 1994).

The research conducted by Pell (1967), Kirk (1967), and Bazin and Saunier (1967) indicated that aggregate gradation has little effect on fatigue performance that can not be explained by differences in asphalt content and air void content of the mixes.

Loading

Loading amplitude, shape and duration of the loading pulse have direct impact on the fatigue life of asphalt mixtures. In both stress controlled and strain controlled loading modes, the higher loading amplitude leads to less fatigue life. Table 2.1 shows the effect of shape of wave form on fatigue life. Under same temperature and loading amplitude, the highest fatigue life was obtained with triangle waveform and square waveform produced the lowest fatigue life. Based on the traffic load, 0.04 to 0.1 second is appropriated for fatigue testing (Figure 2.7).

Table 2.1 Effect of Shape of Waveform on Fatigue Life
(Raithby and Sterling, 1972)

Waveform	Temp, °C	Stress Amp MN/m²	Initial Strain Amp'	Geometric Mean Fatigue Life, Cycles	Relative Lives
⊓⊔	25		1.7×10^{-4}	24,690	0.42
∿	25	±0.33 (48 psi)	1.2×10^{-4}	58,950	1.0
◁▷	25		0.67×10^{-4}	85,570	1.45
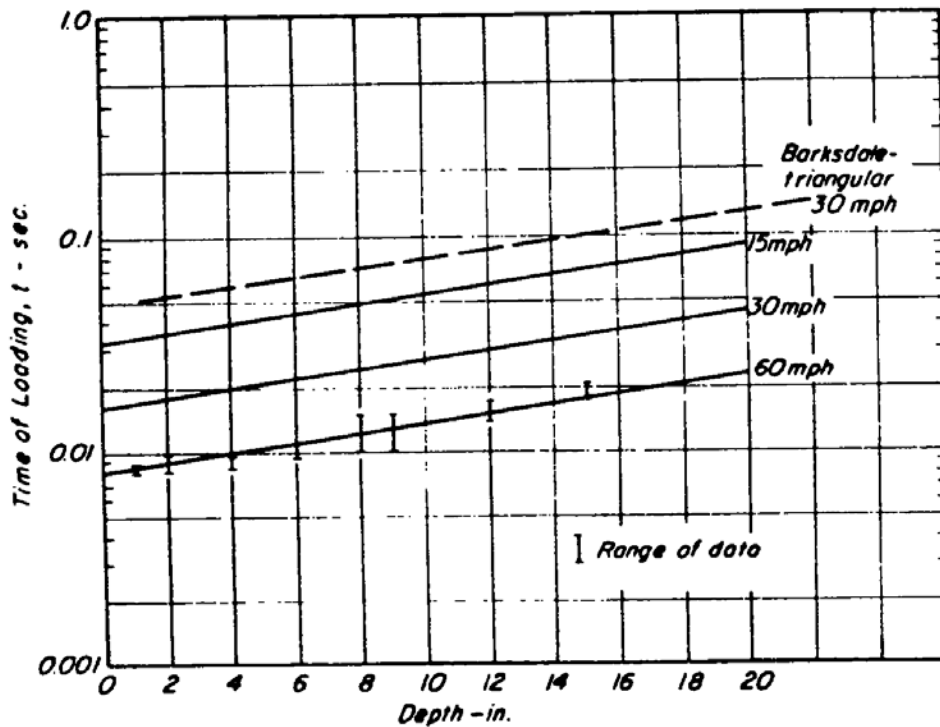
Figure 2.7 Equivalent Time of Loading-Depth Relationship for Horizontal Stress

(Mclean 1974)

Temperature

The fatigue life of asphalt mixture is greatly affected by environmental temperature. The previous research (Deacon et al. 1994) showed that under strain controlled loading mode, fatigue life of asphalt mixture increased as applied strain decreased and decreased with the decrease of temperature (Figure 2.8). However, in the real condition, strain and temperature at bottom of asphalt layer changes at same time. Combining fatigue testing results with mechanistic analysis, Deacon et al. (1994) summarized effects of temperature and temperature gradient on fatigue life of asphalt layer in Figure 2.9. It can be seen that, at moderate temperature, asphalt layer has lowest fatigue life. Temperature gradient also affects fatigue life. Generally, with the increase of temperature gradient the fatigue life decreases. This effect becomes weaken as temperature increased, and is negligible when temperature is above 40°C.

20
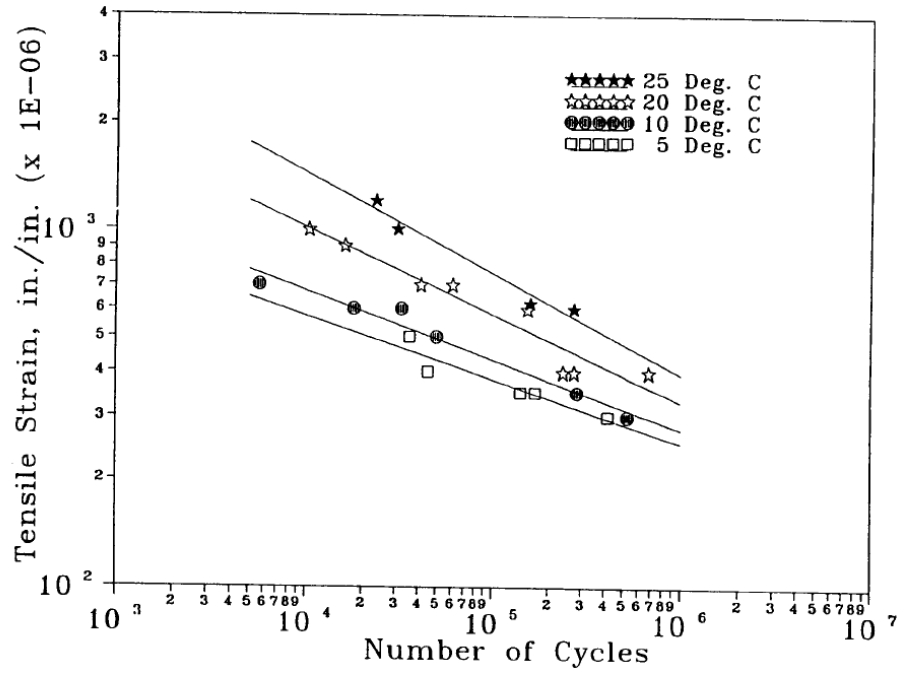
Figure 2.8 Effect of Temperature on Fatigue Life
(Strain Controlled Mode) (Deacon et al. 1994)
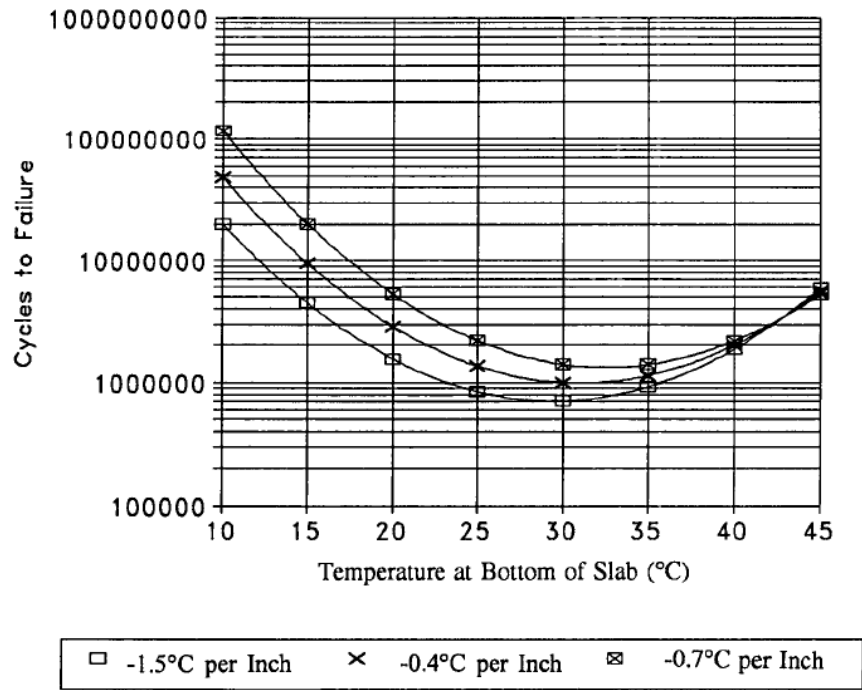
Figure 2.9 Effects of Temperature and Temperature Gradient on Fatigue Life of Asphalt Layer,

(8 in. pavement) (Deacon et al. 1994)

Models

During last several decades, fatigue models have been developed considering influencing factors to predict fatigue performance and incorporate fatigue properties of material into pavement design process.

It has been well accepted that the simple relationship between fatigue life and loading level can be expressed as Equation 2.14 and 2.15 (Pell 196**7**, Monismith et al. 1966). Later, Monismith et al. (1985) suggested that a relationship expressed by Equation 2.16 which is more applicable to asphalt-aggregate mixes in general.

$$N_f = a(\frac{1}{\sigma_0})^b \qquad (2.14)$$

or

$$N_f = a(\frac{1}{\varepsilon_0})^b \qquad (2.15)$$

$$N_f = a(\frac{1}{\varepsilon_0})^b (\frac{1}{S_o})^c \qquad (2.16)$$

where,

N_f = fatigue life,

σ_o = controlled stress,

ε_o = controlled strain,

S_o = initial mix stiffness and

a, b, c = regression constants.

Other approach used for describing fatigue behavior is the total or, cumulative, dissipated energy to failure. Under sinusoidal loading condition, the model can be expressed as Equation 2.17:

$$N_f = a(\psi)^b (\varepsilon_0)^c (S_0)^d (\sin \phi_0)^e \qquad\qquad (2.17)$$

where,

N_f	= fatigue life,
ψ	= energy ratio factor,
ε_o	= controlled strain,
S_o	= initial mix stiffness
ϕ_o	= phase angle, and
a, b, c, d, e	= regression constants.

Van Dijk and Visser (1977) and Tayebali et al. (1992) have shown that the coefficients, "a" to "e", in Equation 2.17 were mix dependent. Therefore, surrogate fatigue models have been proposed by incorporating the basic mixture properties (Equation 2.18)

$$N_f = 466.4e^{0.052VFB} (\varepsilon_0)^{-3.948} (S_0^{"})^{-2.270} \qquad\qquad (2.18)$$

where,

N_f	= fatigue life,
VFB	= percent voids filled with bitumen,
ε_o	= controlled strain, and
$S_o^{''}$	= initial loss stiffness.

RUTTING RESISTANCE

Rutting is the surface depression in the wheel paths induced by repeated traffic load. Rutting is the accumulation of surface wearing and permanent deformation in any of the pavement layers or in the subgrade. In a well constructed road structure, rutting is primarily confined in asphalt layers (White et al.

2002) caused by densification and shear flow (Brown et al. 2009). Numerous studies have been conducted to characterize the rutting resistance of asphalt materials.

Testing Method

Several laboratory testing methods have been developed for rutting characterization, including load wheel test, Superpave shear test, and flow number and flow time test.

Load Wheel Test

Currently, the load wheel tester (LWT) is the most common type of laboratory test used to evaluate the rutting resistance of asphalt mixtures. Several LWTs are being used in the United States, in which Asphalt Pavement Analyzer (APA) and Hamberg Wheel Tracking Device (HWTD) are the most popular ones. The results from both tests show good correlations with in site rutting depth of asphalt layers. During the test, repeated loading is applied on specimen through a loaded wheel tracking back and forth, which simulates the traffic loading on the real pavement. The permanent deformation of specimen is measured at certain number of load cycles.

The APA is a modification of the Georgia Loaded Wheel Tester (GLWT). A wheel is loaded onto a pressurized linear hose (690KPa) and applies a 445N force over a testing sample tracking back and forth to induce rutting. Most testing is carried out to 8,000 cycles and samples also can be tested submerged in water (Kandhal and Cooley 2003).

Testing in the HWTD is conducted under water a 705-N force is applied onto a 47-mm-wide steel wheel. The steel wheel is then tracked back and forth over the slab sample. 20,000 passes are loaded or until 20 mm of deformation occurs (Aschenbrener 1995).

Superpave Shear Test

The Superpave Shear Tester (SST) is a closed-loop servo-hydraulic system that can apply biaxial loads using its dual actuators (Figure 2.10). SST simulates the comparatively high shear stresses that exist near

the pavement surface at the edge of vehicle tires. These stresses lead to lateral and vertical deformations associated with permanent deformation in the surface layers (Witczak 2002). During the testing, the vertical actuator applies vertical axial force and horizontal actuator moves the shear table applying shear loads. The repeated shear at constant height (RSCH) and the frequency sweep at constant height (FSCH) tests can be conducted with SST on a short cylinder specimen (150mm in diameter and 50mm in height). During RSCH test, repeated shear pulses are applied onto the specimen a controlled atmosphere and FSCH test applies repeated shear in a range of loading frequencies. Results from the RSCH test are used to determine the accumulation of permanent shear strain with load repetitions. Results from the FSCH test are used to determine the sample's complex shear modulus (G*) and phase angle (φ). These characteristics can then be used to predict a mixture's permanent deformation potential.
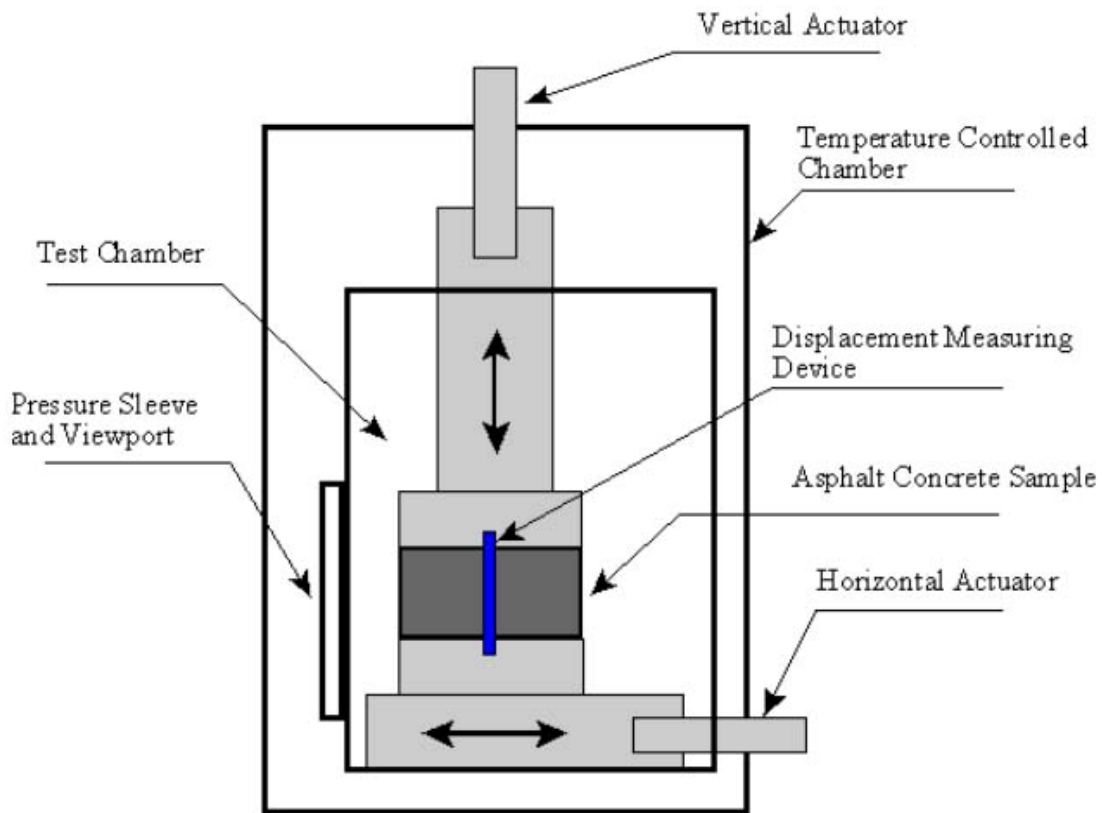
Figure 2.10 Schematic of Superpave Shear Tester

Flow Number and Flow Time Tests

The flow number (FN) test and flow time (FT) test are uniaxial compression tests (Bonaquist 2003). Both tests can be performed with or without confining pressure. In FN test, a load cycle consisting of a 0.1s haversine pulse load and a 0.9 s rest time is repeatedly applied for the test duration at the desire stress level. This load is repeated to 10,000 cycles or until the specimens fail. The test results offer the number of load cycles before material flows and the permanent strain growth model used in the MEPDG. FT test simulates a stationary heavy vehicle on a pavement structure. During the test, a constant load is applied onto the specimen until flow occurs. The duration of the time is called flow time.

Influencing Factor

Temperature

The previous studies (Collins et al. 1995, Collins et al. 1996, Kandhal and Cooley 2003) concluded that temperature has the most pronounced effect on the rutting depth. As temperature increases, rutting depth increases, because at higher temperatures, the asphalt binder becomes less viscous. Testing results obtained using APA at a testing temperature, which corresponds to the high temperature of the PG for a project location, better predicted the field rutting performance than the results obtained at 6°C higher than the high temperature of the PG.

Air voids

Collins et al. (1995) indicated that for a given mixture and test temperature, as the air void content increased, the measured rut depth increased (Figure 2.11). It has been wildly accepted that the air void of specimen used for rutting tests should be around 7 percent, because this air void content generally represents normal construction as well as specified values.
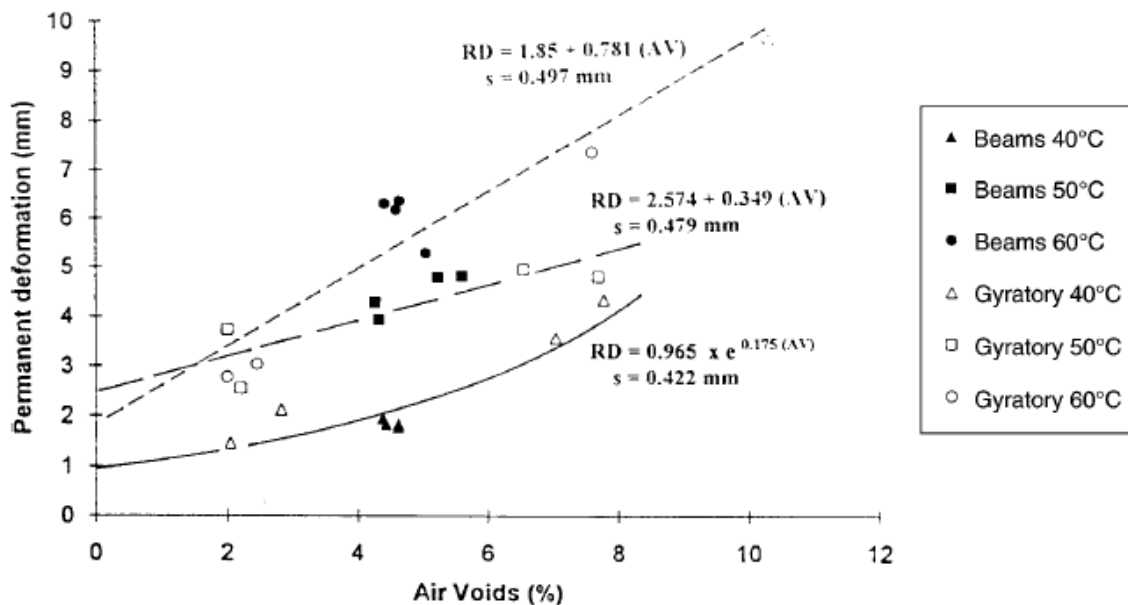
Figure 2.11 Rut Depth versus Air Voids of Beam Samples and Gyratory Samples

(Collins et al. 1995)

Binder

The type of asphalt binder plays an important role on the rutting behavior of mixes. Previous studies (Collins et al. 1995, Netemeyer 1998, Hanson and Cooley 1999, Kandhal and Mallick 1999) indicated that mixes containing stiffer grades of asphalt binder provided lower rut depths. As $G*/\sin\delta$ increased, the rutting potential decreased. Maupin (1998) also showed that, as binder content increased 1% higher than optimum binder content, the measured rut depth increased.

Aggregate

Kandhal and Mallick (1999) conducted a study investigate the effects of gradation and nominal maximum aggregate size (NMAS) on rutting resistance of asphalt mixes using APA. Three types of gradations were used (above, below and through the restricted zone). The results show that, for the granite and limestone asphalt mixes, the gradation passing below the restricted zone had the highest amount of rutting while the gradation passing through the restricted zone generally had the least amount of rutting. However, for the

27

crushed gravel aggregate, the least amount of rutting was obtained with the gradation below the restricted zone and the highest amount was obtained with the gradation above the restricted zone. The studies (Lai 1988, Stuart and Mogawer 1997, Netemeyer 1998, Kandhal and Mallick 1999) also showed that larger NMAS had lower rut depths. In addition, Netemeyer (1998) indicated that increases in natural sand content resulted in higher rutting depth. The results also indicated that increasing the aggregate passing the No. 50 sieve decreased rutting potential and as the aggregate passing the No. 100 sieve increased, the rutting potential increased.

Model

Shami et al. (1997) developed a model to prediction rut depth of an HMA mix with the GLWT for different temperatures and number of loading cycles (Equation 2.19). Based on this model, the testing time for the APA could be reduced by obtaining equal rutting depth with reduced loading cycles at higher temperature. Secondly, the rutting behavior of a particular mix could be predicted for different service conditions and pavement temperatures.

$$\frac{R}{R_0} = \left(\frac{T}{T_0}\right)^{\alpha} \left(\frac{N}{N_0}\right)^{\beta} \qquad\qquad (2.19)$$

where,

R = predicted rut depth,

R_o = reference rut depth obtained from the LWT test at the reference conditions T_o and N_o,

T, N = temperature and number of load cycles at which the rut depth is measured

T_o, N_o = reference temperature and load cycles at the R_o, and,

α, β = regression constants

Based on laboratory test results, constitutive model (Equation 2.20) among permanent strain, temperature and loading cycles has been developed using statistical analysis and adopted in MEPDG.

$$\frac{\varepsilon_p}{\varepsilon_r} = aT^b N^c \qquad\qquad (2.20)$$

where,

ε_p = accumulated plastic strain at N repetitions of load,

ε_r = resilient strain of the asphalt material as a function of mix properties, temperature and time rate of loading,

N = number of load repetitions,

T = pavement temperature, and,

a, b, c   = regression coefficients.

CHAPTER III

LABORATORY INVESTIGATION

This chapter presents details of laboratory testing, including materials selection, specimens fabrication, testing methods and equipment. Properties of materials are summarized as well.

MATERIALS

Aggregate

To characterize engineering properties of typical Alaska ATBs, granular materials used for base course construction, known as D-1 materials, were collected from three regions in Alaska. Figure 3.1 shows samples of D-1 materials from northern, central and southeast regions, respectively. Aggregate properties were tested before asphalt treatments. Those properties included aggregate gradation, abrasion resistance, percent of fractured surface, and percent of flat and elongated aggregate.

Figure 3.1 D-1 Material from Three Regions (from Left: Northern, Central and Southeast Regions)

Table 3.1 presents detailed information of aggregate gradations. As shown in Figure 3.2, the gradations of all D-1 materials were within the range of upper and lower limits of D-1 material specified

in AKDOF&PF's Standard Specification for Highway Construction (SSHC). In addition, their gradations were very close to each other. Therefore, a reference gradation was used by averaging the gradations of aggregates from the three regions. The optimum moisture content for the materials with the reference gradation was 5.3%.

Table 3.1 Gradation of D-1 Materials

Sieve Designation		% Passing					
Standard (mm)	Alternate	Northern Regions	Central Region	Southeast Region	Reference	D-1 Standard	
25	1"	100.0%	100.0%	100.0%	100.0%	100.0%	100.0%
19	3/4"	97.6%	99.6%	100.0%	100.0%	70.0%	100.0%
9.5	3/8"	74.2%	72.6%	69.1%	72.4%	50.0%	80.0%
4.75	#4	47.3%	50.0%	41.8%	46.7%	35.0%	65.0%
2.36	#8	30.4%	37.5%	25.4%	31.3%	20.0%	50.0%
0.3	#50	11.2%	9.9%	8.1%	9.8%	8.0%	30.0%
0.075	#200	2.7%	2.9%	3.9%	3.2%	0.0%	6.0%
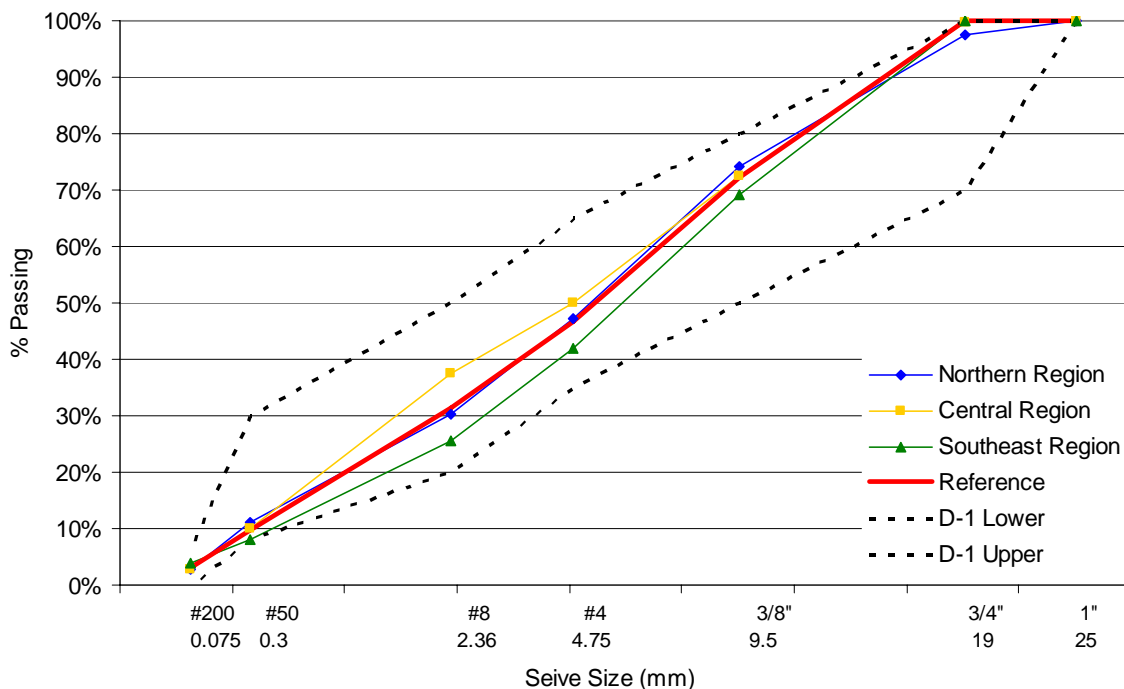
Figure 3.2 Gradation of D-1 Materials

The abrasion resistance tests were conducted using the Micro−Deval apparatus (Figure 3.3) according to AASHTO T327-1, which is a measure of abrasion resistance and durability of mineral aggregates resulting from a combination of actions including abrasion and grinding with steel balls in the presence of water. The result is presented by the percent loss of aggregate passing 1.18 mm (No. 8) sieve after abrasion. The lower percent loss, the better abrasion resistance of aggregate.

Figure 3.3 Micro−Deval Apparatus

Flat or elongated particles test determines the percentages of flat particles, elongated particles, or flat and elongated particles in coarse aggregates according to ASTM D4791. If the elongated ratio of maximum dimension to the minimum dimension of an aggregate particle is 5:1 or over, it is defined as an elongated particle. The test result is presented by the percentage of the particles over the entire sample by mass. Figure 3.4 shows the device used to perform this test.

Percent fractured face test was used to determine the percentage, by mass, of coarse aggregates that consist of fractured particles according to ASTM D5821. If an aggregate particle contains one fractured face, it is considered as a fractured particle.

Figure 3.4 Measuring Caliper for Flat or Elongated Particles Test

Table 3.2 summarizes properties of D−1 materials from three regions and requirements in SSHC. It can be seen from Table 3.2, D−1 materials from northern region had the best abrasion resistance among all three regions and materials from southeast region had the lowest one. 100% particles of D−1 material from southeast region had at least one fractured surface, while the percentages of fractured surface for central and northern region were 91.7% and 84.5%, respectively. D−1 material from southeast region contained 3% flat and elongated particles and none of them were found in materials from central and northern regions.

Table 3.2 Engineering Properties of D−1 Materials

Source	Abrasion Resistance (% Loss)	Percent Fractured Face (one fractured face, %)		Flat or Elongated Pieces (5:1, %)	
		Test Results	Requirement	Test Results	Requirement
Southeast Region	9.7	100	≥80	3	≤8
Central Region	5.8	91.7		0	
Northern Region	2.7	84.5		0	

Asphalt Binder

The asphalt binder used for this study was PG 52-28 asphalt, which is the neat asphalt type used in Alaska. Three binder contents, 2.5%, 3.5% and 4.5% by weight of total mixture were introduced to prepare specimens of HATB. The PG 52-28 binder was also used to generate foamed asphalt with the WLB 10 foamed asphalt laboratory system (Figure 3.5) to prepare FATB specimens, and the percentages of foamed asphalt (residual binder) applied to FATB were 1.5%, 2.5%, and 3.5% in this study. The type of emulsified asphalt used in this study to prepare EATB specimens was CSS-1, a cationic emulsion with low viscosity. The percentages of emulsion added were 1.5%, 2.5%, and 3.5% of residual binder.

Figure 3.5 WLB 10 Foamed Asphalt Laboratory System

SPECIMENS FABRICATION

Cylindrical Specimens for Triaxial Test

Cylindrical specimens were fabricated with three kinds of ATBs for triaxial tests. For HATB, loose mixtures were compacted by the Superpave gyratory compactor (SGC), producing specimens with 6 inches in diameter and 7 inches in height. The specimens were then cored and sawed (Figure 3.6) to the required dimensions: 4-in in diameter and 6-in in height (Witczak et al. 2000). In AKDOT&PF's SSHC, it is required to compact HATBs to a minimum density of 94% of the maximum specific gravity, which equals to a 6% maximum air voids content. Therefore, 6% was selected as the control target air voids content for all HATB specimens. To achieve this target, higher compaction effort were applied to specimens with lower binder content. For specimens with 2.5% binder content, during the compaction, the number of gyration could go up to 150. For specimens with 4.5% binder content, only 20 gyrations were applied.

The loose foamed asphalt mixtures were prepared at AKDOT&PF's central region material lab and then shipped back to AUTC lab for compaction. 1% portland cement by weight of aggregate was introduced to enhance the strength of FATB and act as an anti-strip additive. Specimens were directly compacted to the final size, which was 4-in in diameter and 6-in in height (Figure 3.7), using the modified compaction effort according to ASTM D1557.

Figure 3.6 HATB Specimens for Triaxial Test

Figure 3.7 FATB Specimens for Triaxial Test

Cylindrical specimens of EATB were compacted at the "pseudo optimum" moisture content. At each emulsion content, the "pseudo optimum" moisture content of FATB was determined by the density vs. moisture content curve from the compaction test after adding emulsified asphalt to the granular D-1 materials.

Cylindrical specimens made with a combination of 50% D-1 materials and 50% of reclaimed asphalt pavement (RAP) were also prepared for M_R and permanent deformation tests. The optimum moisture content was 5% according to the test result of the compaction test illustrated in Figure 3.8. The triaxial test was performed on specimens with 4 in. in diameter and 8 in. in height at the optimum moisture content. To prevent water evaporation, the specimens were covered with rubber membrane and aluminum foil after ejecting from the molds before testing (Figure 3.9).
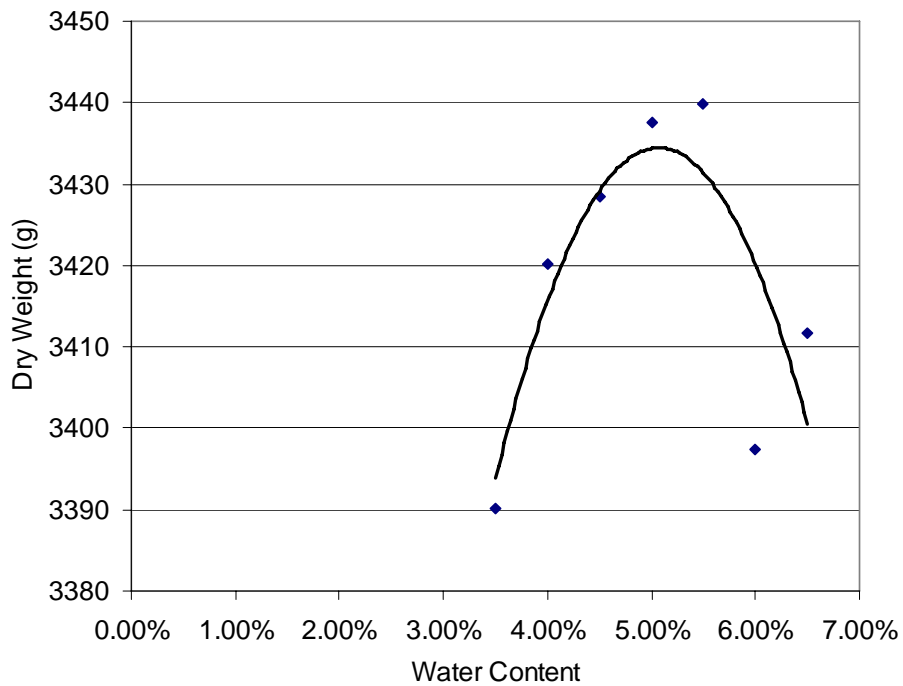
Figure 3.8 Compaction Test Result of Specimens Made with RAP

Figure 3.9 ETAB Specimens after Compaction

Beam Specimens for Fatigue Test

Beam specimens were prepared for fatigue tests. For HATB beam specimens, loose materials with D-1 materials from three regions at two binder contents, i.e., 3.5% and 4.5%, were compacted to 4×4 ×16 in. beam by a kneading compactor (Figure 3.10). Then beams were cut into final size, which was 2×2.5×15 in (Figure 3.11). There were six replicates for each mix, with a total of 36 beams specimens for materials from three regions. Due to the low bonding effects, beam specimens could not be manufactured for EATB, FATB and HATB with 2.5% binder content.

Figure 3.10 Kneading Compactor for Preparing Beam Specimens
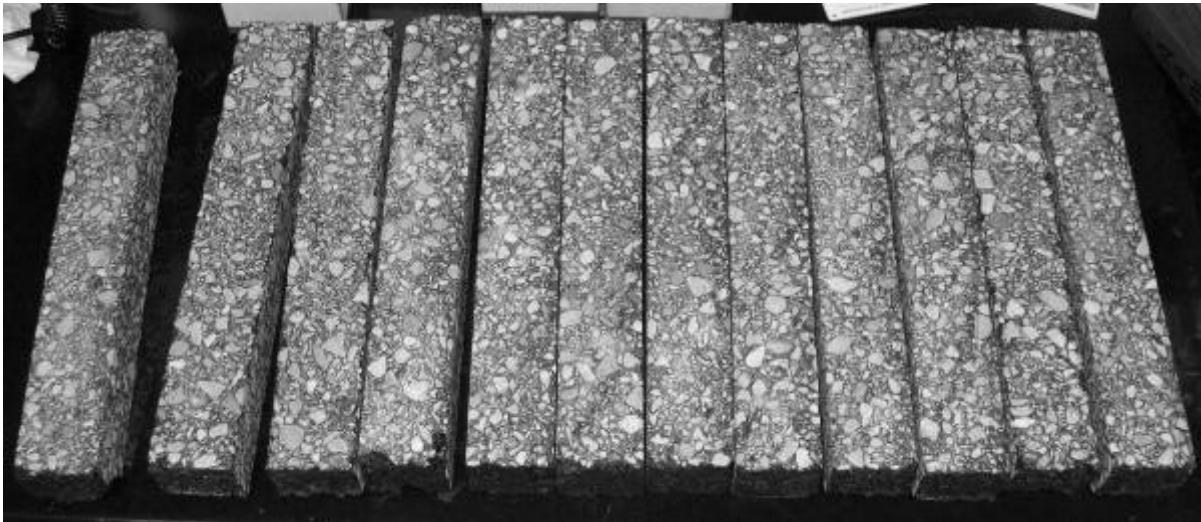
Figure 3.11 Beam Specimens for Fatigue Test

Cylindrical Specimens for Rutting Test

Totally 36 cylindrical HATB specimens were made for rutting test. Three binder contents, i.e. 2.5%, 3.5% and 4.5%, were used for D-1 materials from three regions. Four specimens were made for each set. Cylindrical specimens were compacted by the SGC in a 6-in diameter mold with a height of 3 inches. The target air voids content of specimens treated with 3.5% and 4.5% of asphalt was same as those for triaxial tests, which was 6%. However, specimens treated with 2.5% binder content could not reach this target due to the extremely low binder content.

LABORATORY TESTS

The laboratory tests conducted in this study included 1) M_R and permanent deformation tests of HATBs, FATBs, EATBs and RAP specimens; 2) beam fatigue tests for HATBs, and 3) rutting tests for HATBs. Table 3.3 lists the overall experimental design in this study.

M_R and permanent deformation tests

As summarized in literature review, there are two candidate methods to perform M_R and permanent deformation tests: triaxial test and indirect tensile test. Considering that ATBs are light bond material, especially for EATB and FATB, thin cylindrical specimens are fragile and would fall a part before or during the indirect tensile test. On the other hand, indirect tensile test is not capable to investigate the effects of confining pressure (Barksdal et al. 1997, Fu and Harvey 2007), which is a mainly influencing factor on the M_R. Therefore, the triaxial test method was adopted for this study.

Table 3.3 Overall Experimental Design

Mixture types	Binder grade	Aggregate	Binder Content	Resilient modulus & Permanent Deformation	Rutting	Beam Fatigue
HATB	PG 52-28	D1-1	2.5%	3×3	4	-
			3.5%	3×3	4	2×3
			4.5%	3×3	4	2×3
		D1-2	2.5%	3×3	4	-
			3.5%	3×3	4	2×3
			4.5%	3×3	4	2×3
		D1-3	2.5%	3×3	4	-
			3.5%	3×3	4	2×3
			4.5%	3×3	4	2×3
EATB	CSS-1	D1-1	1.5%	3×3	-	-
			2.5%	3×3	-	-
			3.5%	3×3	-	-
		D1-2	1.5%	3×3	-	-
			2.5%	3×3	-	-
			3.5%	3×3	-	-
		D1-3	1.5%	3×3	-	-
			2.5%	3×3	-	-
			3.5%	3×3	-	-
FATB	PG 52-28	D1-1	1.5%	3×3	-	-
			2.5%	3×3	-	-
			3.5%	3×3	-	-
		D1-2	1.5%	3×3	-	-
			2.5%	3×3	-	-
			3.5%	3×3	-	-
		D1-3	1.5%	3×3	-	-
			2.5%	3×3	-	-
			3.5%	3×3	-	-
50:50 mixture of RAP and D-1 base	-	D1-1	-	3×3	-	-
		D1-2	-	3×3	-	-
		D1-3	-	3×3	-	-

*Note: * D1-1, D1-2, and D1-3 represent 3 D-1 base course materials.*

* Numbers in cells represent the number of samples tested. Resilient modulus was tested under 3 different temperatures and beam fatigue was tested under 3 different loading levels.

The M_R and permanent deformation test was performed on a close-loop testing system with a temperature chamber (Figure 3.12) according to the standard of AASHTO T307. Two Linear Variable

Differential Transducers (LVDTs) were used to measure the deformation of ATB specimens. They were located on clamps at ¼ points of specimen to eliminate the measuring influence due to the loading rod deformation and end restrain effect of load ram (Barksdale et al. 1997). The loading sequences, as shown in Table 3.4 and Figure 3.13, included a conditioning sequence and 15 loading sequences under 5 different confining pressures (i.e. 3, 5, 10, 15 and 20 psi, respectively). For each confining pressure, 3 different axial loads were applied to specimen. The conditioning loading consisted of 1000 loading cycles which were applied at confining pressure of 15 psi and maximum axial stress of 15 psi. This sequence was designed to eliminate the effects of the interval between compaction and loading and eliminate the initial loading versus reloading. The conditioning also aided in minimizing the effects of initially imperfect contact between the loading ram and sample cap, as well as base plate and the test specimen.

Figure 3.12 Resilient Modulus and Permanent Deformation Testing System

The data of the last five load cycles of each loading segment were recorded to calculate M_R. A typical testing data segment is shown in Figure 3.14. The recoverable strain was defined as maximum deformation strain minus minimum deformation strain at each loading cycle. The total unrecoverable strain during the whole loading process was calculated as the permanent deformation.

Table 3.4 Loading Consequences of Triaxial Test

Consequences	Confining Pressure (psi)	Deviator Stress (psi)
0	15	15
1		3
2	3	6
3		9
4		5
5	5	10
6		15
7		10
8	10	20
9		30
10		10
11	15	15
12		30
13		15
14	20	20
15		40

Figure 3.13 Loading Consequences of Triaxial Test
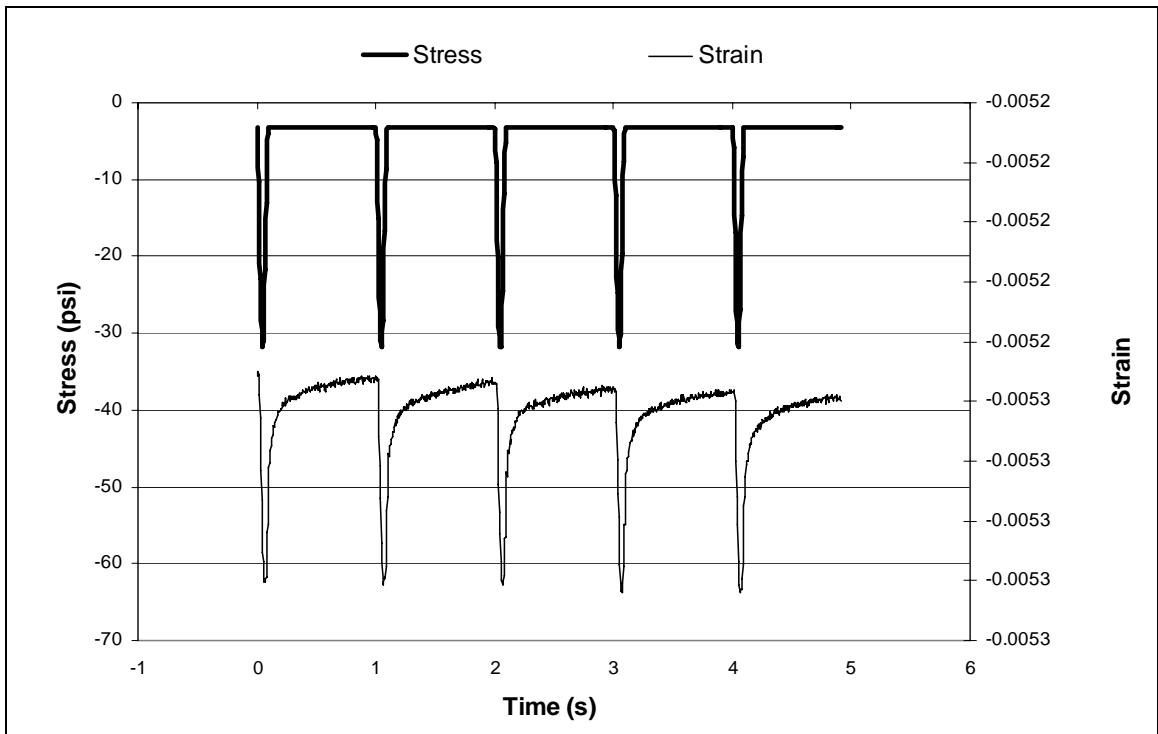
Figure 3.14 Typical Resilient Modulus Testing Data Segment

Beam fatigue test

Repeated flexural test (Figure 3.15) was used to investigate the fatigue performance of HATB specimens with controlled strain loading mode. Beam specimens of FATB and EATB were too fragile to be tested by this method. During the test, repeated haversine loads were applied at the one-third points of a beam specimen at 10 Hz. This produced a constant bending moment over the center portion of the beam. Under the strain controlled loading mode, to maintain a constant bending strain, the applied force gradually decreased. Usually, the fatigue life of beam specimens is defined as the number of loading cycles at which the flexural modulus of specimen reduces to 50% of the initial value. The initial value of modulus is measured at the 50th loading cycle. The beam fatigue tests were performed at three different strain levels. The influence of binder content was also investigated during this test. However, because HATBs with 2.5% binder content were too fragile to make beam specimens, only those made with 3.5% and 4.5% binder content were used for fatigue tests.

Rutting

Rutting tests were conducted by using the Georgia Loader Wheel Tester (Figure 3.16). During this test, repeated wheel loads were applied on the surface of biscuit specimens though pressurized rubber hoses. For each mix, four specimens were used for the tests. Initial 25 loading cycles were applied to force specimens sitting firmly in the holding device. The rut depths were measured after the next 8000 cycles were applied and an average value was used to represent the final rut depth of each mix. The test may stop when the rut depth exceeded 13mm, which was out of measuring range of the gauge. HATBs with three binder contents, 2.5%, 3.5% and 4.5% were tested. However, no data was available for EATB specimens, as the rut depth of EATB specimens already exceeded the measuring range after the initial 25 loading cycles.
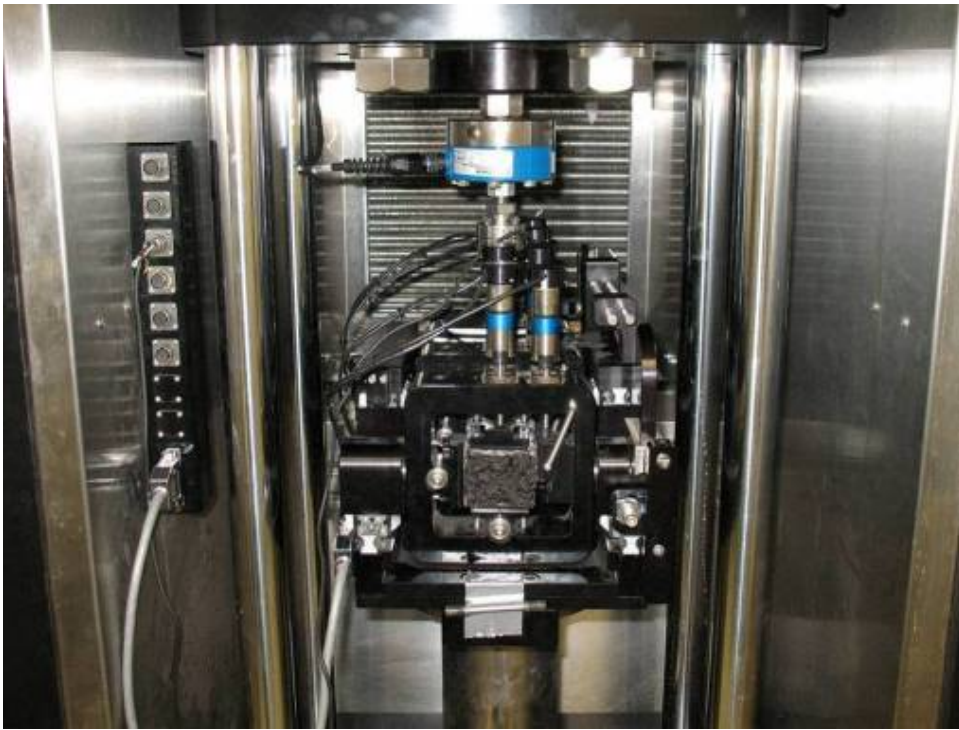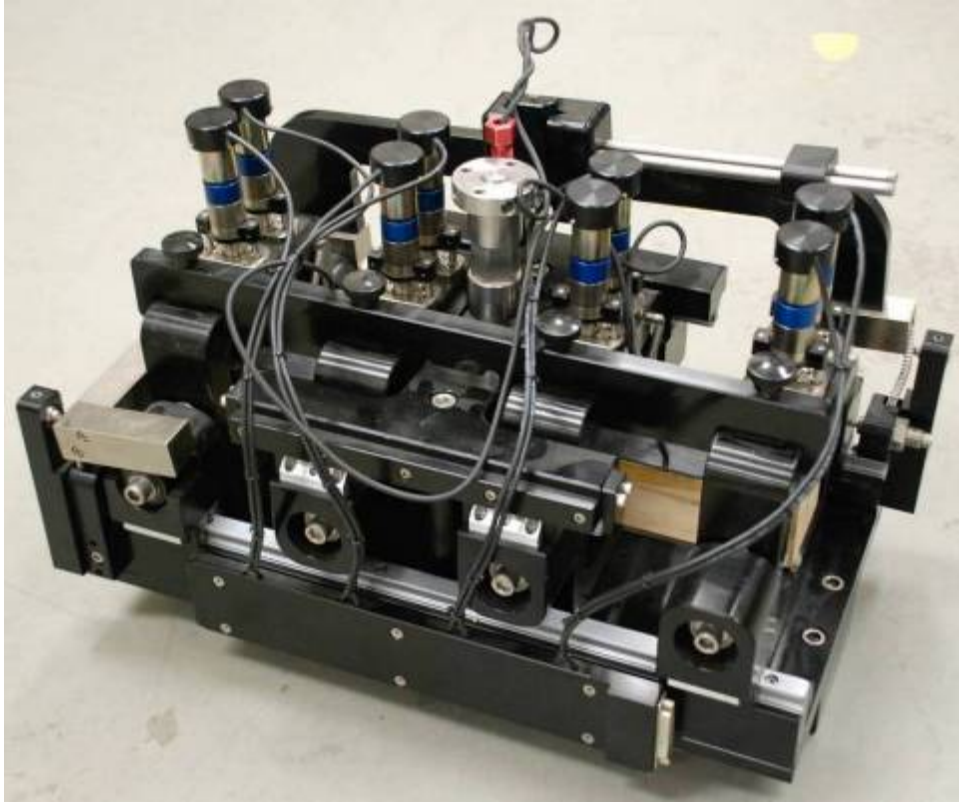
Figure 3.15 Beam Fatigue Testing Equipment

Figure 3.16 Georgia Loader Wheel Tester

CHAPTER IV

TESTING RESULTS

In this study, repeated triaxial test, rutting test and fatigue test were performed to characterize typical Alaska ATBs. This chapter presents the testing results and data interpretation. Triaixal tests were conducted on three kinds of ATBs and a mixture of RAP and D-1 materials at 50%:50% ratio. M_Rs were calculated based on triaxial test results. Effects of temperature, binder content, stress state and aggregate source on resilient modulus were investigated. M_R predicting models were developed for ATBs considering these influencing factors. Rutting and fatigue tests were only performed on HATB specimens and results were summarized as well.

M_RS OF ATBS

Triaxial tests were performed to characterize the resilient behavior of ATBs and effects of influencing factors. The detailed testing results were summarized in Appendix. Table 4.1 compares the typical M_R values of RAP (50:50), EATB (3% residual binder content) and HATB (4% residual binder content) in the AKFPD software and measured values from this study. The typical values were obtained from in-service roadways through falling weight deflectometer (FWD) tests and back-calculation. Compared with those typical values (single values at different seasons), the measured M_R of ATBs varied within a wide ranges under different binder contents, aggregate sources, and stress states at certain temperature. The data also shows that, at lower temperature, compared to the laboratory measured values, moduli of ATBs were under estimated by back-calculation. At 20^oC, M_Rs of EATB obtained through triaxial tests are also much higher than recommended summer & fall value. For RAP (50:50), the triaxial tests were performed on

specimens at optimum moisture content (OMC). At 20°C, the measured moduli were lower than recommended summer & fall value.

Table 4.1 Comparison between Measured M_R and Recommended Values

Typical M_R in Alaska Flexible Pavement Design Manual (ksi)				Measured M_R Range (ksi)			
Material Type	Winter	Spring	Summer & Fall	Material Type	-10°C	0°C	20°C
RAP(50:50)	115	80	80	RAP(50:50)	550-4000	600-1165*	15-61
EATB, 3% Emulsion	115	75	75	EATB, 3.5% Emulsion	1361-3846	1079-2888	197-535
HATB, 4% Asphalt	1500	250	250	HATB, .4.5%, Asphalt	1400-5250	700-4600	200-900
				FATB, 3.5% Asphalt Residual	120-400	45-360	30-220

* The triaxial tests were performed at -2°C.

Hot asphalt treated base

As shown in Figure 4.1, temperature greatly influenced the resilient modulus of HATB. When ambient temperature dropped from 20°C to -10°C, at highest bulk stress level, the modulus increased from 500ksi to 2900ksi, almost 4 times higher. The temperature sensitivity of ATBs was mainly contributed by the property of asphalt. Asphalt is temperature sensitive in nature. With the decrease of temperature, the stiffness of asphalt dramatically increases. In HATB, all mineral particles were well coated by asphalt film, which provided great bounding effort to hold all particles together. Decrease of temperature enhanced the bounding effect by increasing the stiffness of asphalt, leading to a great increase of modulus over all specimens.
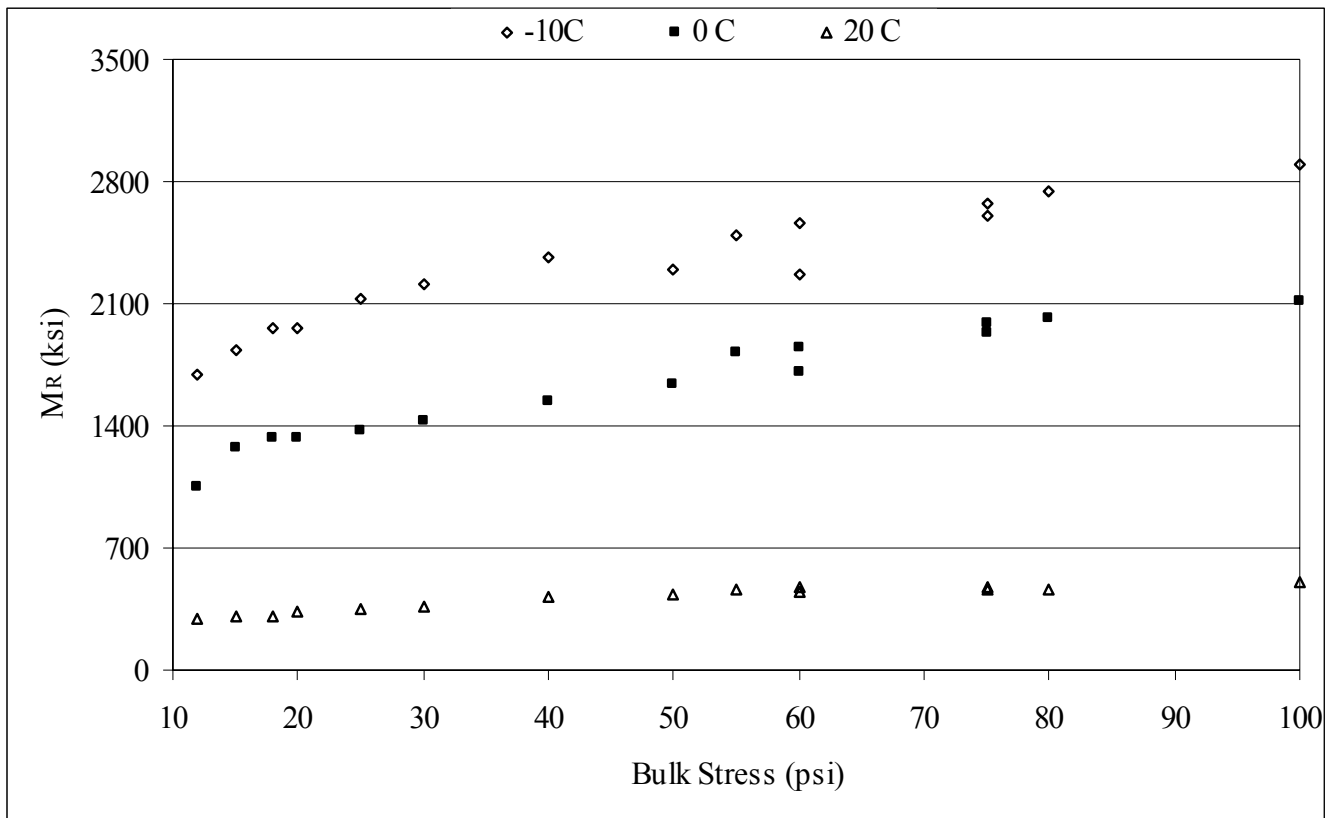
Figure 4.1 Effects of Temperature on M_R of HATB

(Northern region, 3.5% Binder)

For HATB, binder content is one of the primary affecting factors. Using HATB made with D-1 materials from Northern regions as an example, lower binder content produces higher modulus (Figure 4.2). This finding correlated to that obtained by the predictive equations in previous studies (Terrel and Awad 1972, ARA, Inc. 2000), which indicated that the modulus of asphalt mixture decreased as the binder or effective binder content increased. In addition, as required in AKDOT&PF Standard Specifications for Highway Construction (Green 2004), air voids of all HATB specimens with different binder contents were controlled at 6% in this study. To meet this requirement, higher compaction efforts were applied to specimens with lower binder contents. At 2.5% binder content, gyration numbers went up to 150, while only 20 gyrations were applied to specimens with 4.5% binder content. Higher compaction efforts applied to specimens with lower binder contents contributed to higher M_R values of HATB as well. During compaction, higher compaction efforts were applied to specimens with lower binder content. At 2.5%

binder content, the gyration number went up to 150 and only 20 gyrations were applied to specimens with 4.5%binder content. In addition, 2.5% is a very low binder content, but during the mixing process, aggregates were still well coated by asphalt film. The value of M_R at 2.5% is almost three time of the value at 4.5%.
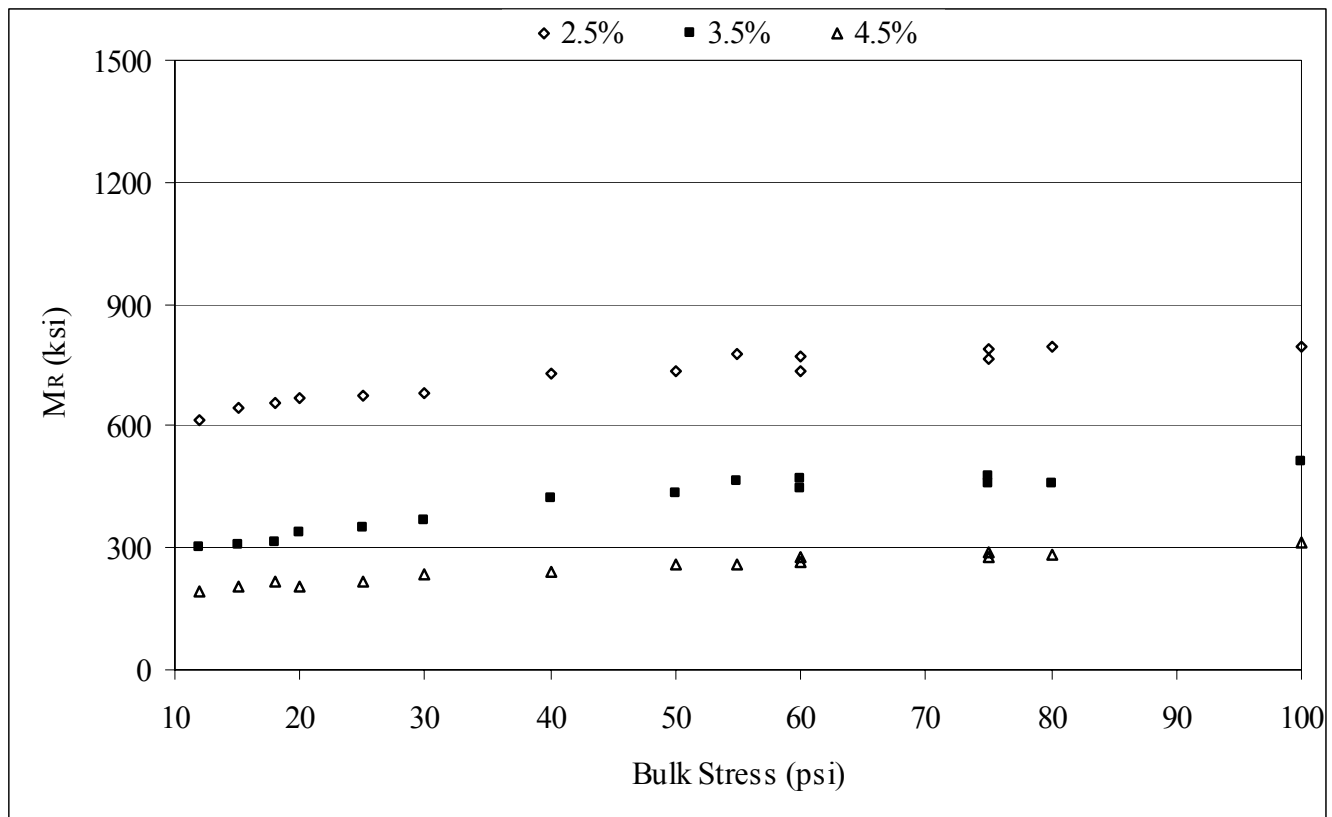
Figure 4.2 Effects of Binder Content on M_R of ATBs
(Northern region, 20°C)

In Figure 4.3, compare to the factors such as binder content and temperature, the effect of aggregate resource was less significant for HATB. Specimens composed of material form Northern region had the lowest moduli. There was not obvious difference of M_R between those from Southeast and Central region. Three performance tests were conducted during this study to distinguish and evaluate D-1 materials from different regions. However, material with higher abrasion resistance (northern region) did not produce higher M_R. The results indicated that, the surface texture of aggregate had a most significant effect on the modulus of ATBs among three aggregate properties. The connection between individual

particles was the weakest part over the entire components of specimen, which dominate the overall resilient behavior of ATBs. Better surface texture improved the connection by increasing the friction angle.
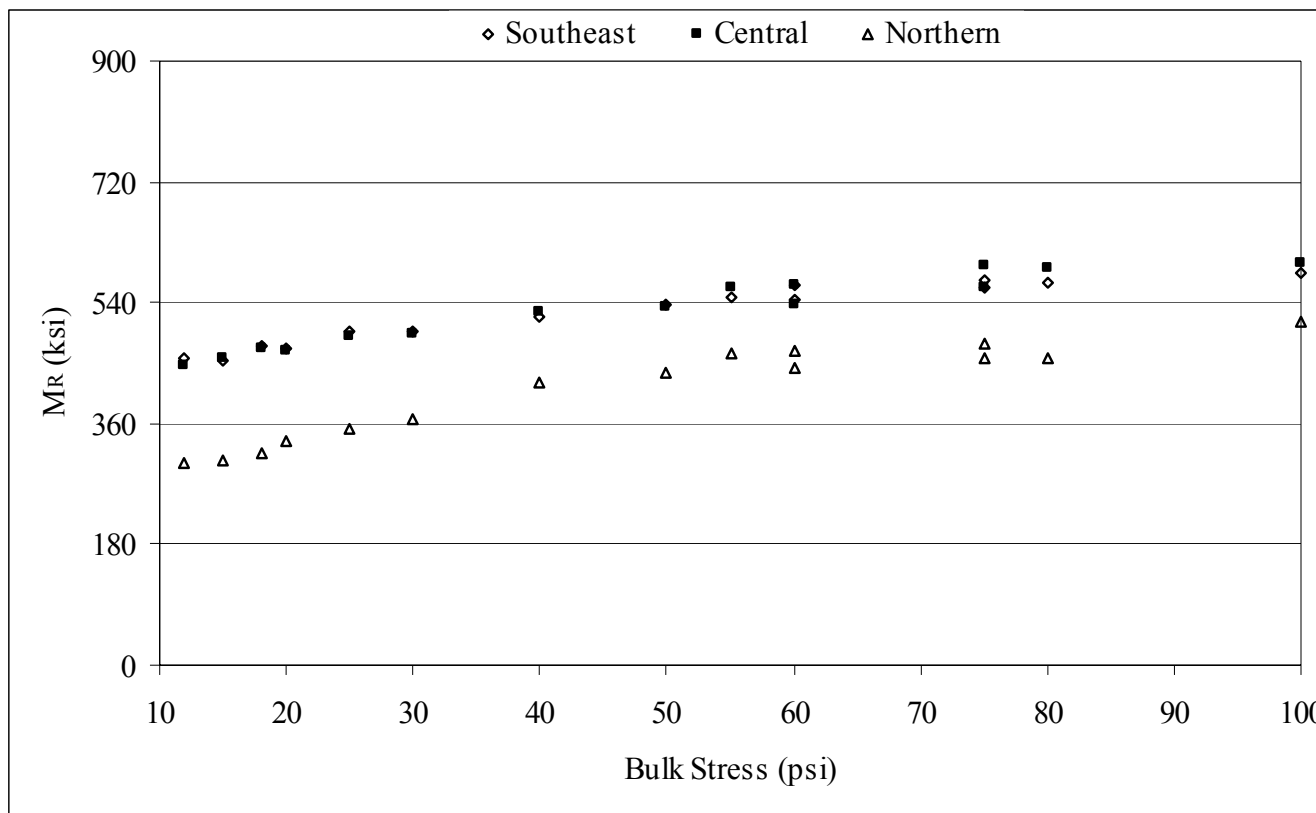
Figure 4.3 Effects of Aggregate Resource on M_R of ATBs
(3.5% binder content, 20°C)

HATB exhibited stress state dependent properties during the triaxial test. Generally, the M_Rs increased with the increase of confining pressure and deviator stress (Figure 4.4). However, at same confining pressure level (especially at higher confining pressure levels), the M_R of HATB didn't increase much with the increase of deviator stress. In this study, the MEPDG model (Equation 4.1) (ARA, Inc. 2000), which was modified from the octahedral stress model, was used to model the behavior of ATBs. Equation 4.1, which can be easily converted into a linear form, was used to perform the multiple linear regression analysis for all M_R data. The values of regression constants, k_1, k_2 and k_3, were obtained for each test through regression analysis based on MEPDG model.

52
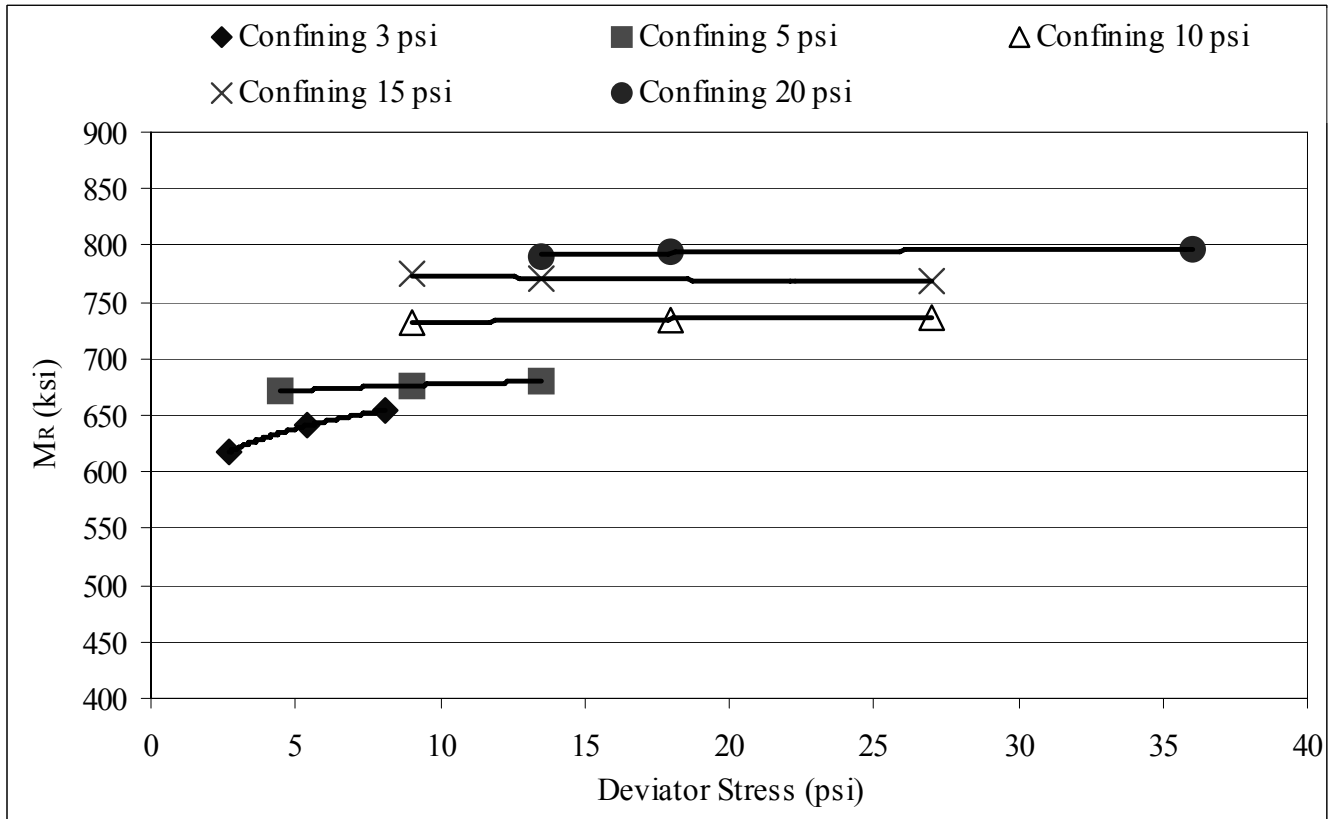
Figure 4.4 Effects of Stress State on M_R of HATB
(2.5% Binder, Northern Region, 20 $^{\circ}$C)

The effects of influencing factors, including aggregate source, temperature, binder content, were also analyzed and integrated into the final predicting model. Through statistical analysis, it was found that for HATB, the value of regression constant k_1 was greatly affected by binder contents, testing temperature and aggregate sources. However, the same effects were not found on regression constants k_2 and k_3. Therefore, the final predicting model for M_R of HATB was developed, as shown in Equation 4.2, in which $k_1 = e^{1.1548+0.04736F-0.0596T-0.1723P_b}$, $k_2 = 0.2669$ and $k_3 = -0.4109$.

$$M_R = k_1 P_a \left(\frac{\theta}{P_a}\right)^{k_2} \left(\frac{\tau_{oct}}{P_a}+1\right)^{k_3} \tag{4.1}$$

$$M_R = e^{1.1548+0.04736F-0.0596T-0.1723P_b} P_a \left(\frac{\theta}{P_a}\right)^{0.2669} \left(\frac{\tau_{oct}}{P_a}+1\right)^{-0.4109} \qquad R^2 = 87\% \tag{4.2}$$

where,

M_R = resilient modulus, ksi,

θ = bulk stress, $\sigma_1+\sigma_2+\sigma_3$, psi,

τ_{oct} = deviatoric stress, $1/3[(\sigma_1-\sigma_2)^2+(\sigma_1-\sigma_3)^2+(\sigma_2-\sigma_3)^2]^{1/2}$, psi,

P_a = atmosphere air pressure, psi, and

k_1, k_2, k_3 = regression constants.

F = fractured surface, %

T = temperature, °C, and

P_b = percent binder by total weight, %.

Emulsified asphalt treated base

Same as HATB, M_R of EATB was also greatly influenced by the ambient temperature. Figure 4.5 shows the temperature effect on Northern region EATB with 3.5% residual binder content. When temperature dropped to -10°C from 20°C, the moduli increased at least 7 times higher. In addition, at lower temperature, specimens were much stiffer that it at higher temperature. Therefore, the deformation was much smaller and hard to be measured precisely, leading to higher variation on M_R of EATBs. It can be seen from Figure 4.5 that, at -10°C the data points spreads out, compare to the data at 20°C.
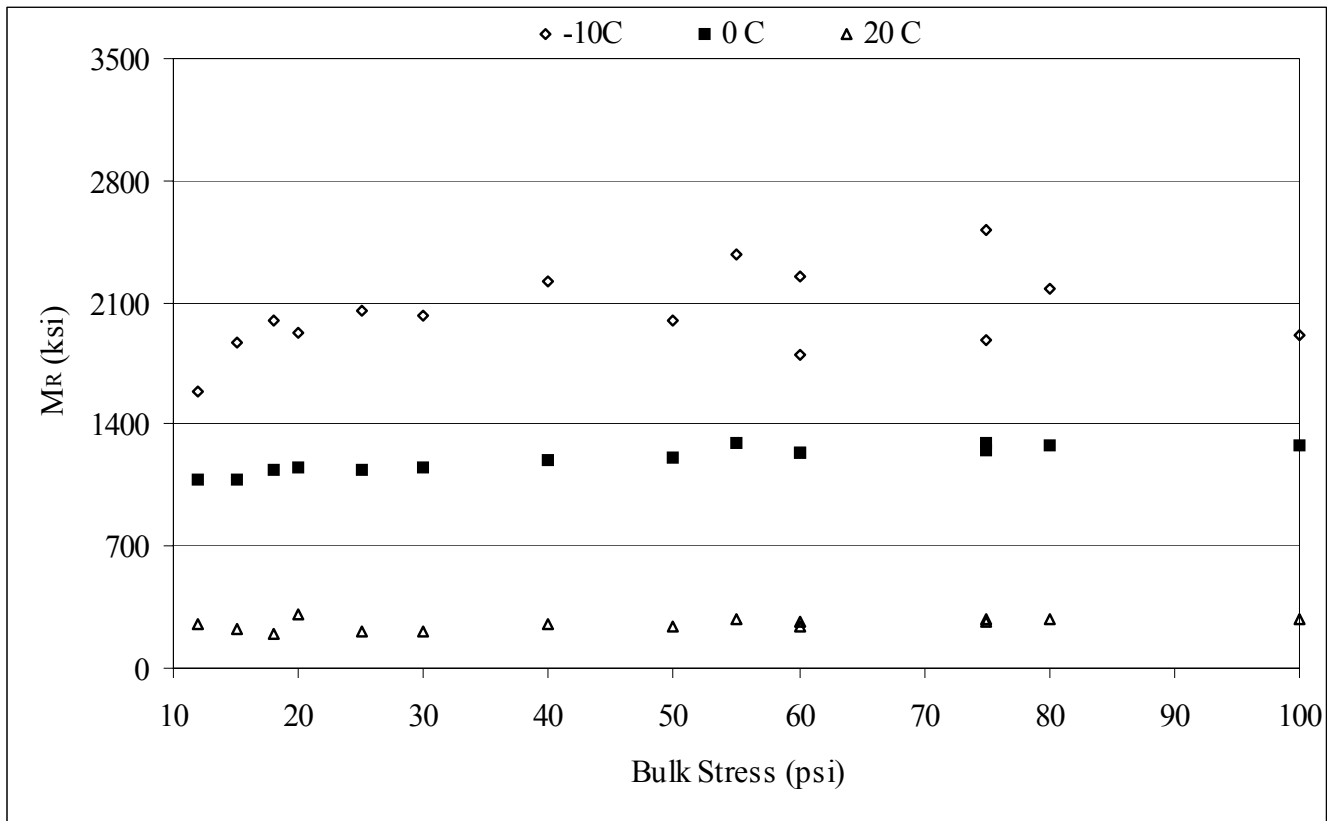
Figure 4.5 Effects of Temperature on M_R of EATB

(Northern Region, 3.5% Residual Binder)

The test results indicated that the M_Rs of EATB did not always increase as residual binder content increased. For example, as shown in Figure 4.6, for materials from Northern region at $20^{\circ}C$, EATB with 1.5% binder content produced higher moduli than those with other two binder contents, which were generally in the range between 300 psi and 400 psi. At higher binder content, the change of residual binder content did not greatly affect the M_R of EATB. In this figure, M_Rs of EATB with 2.5% and 3.5% residual binder contents almost overlapped on each other.
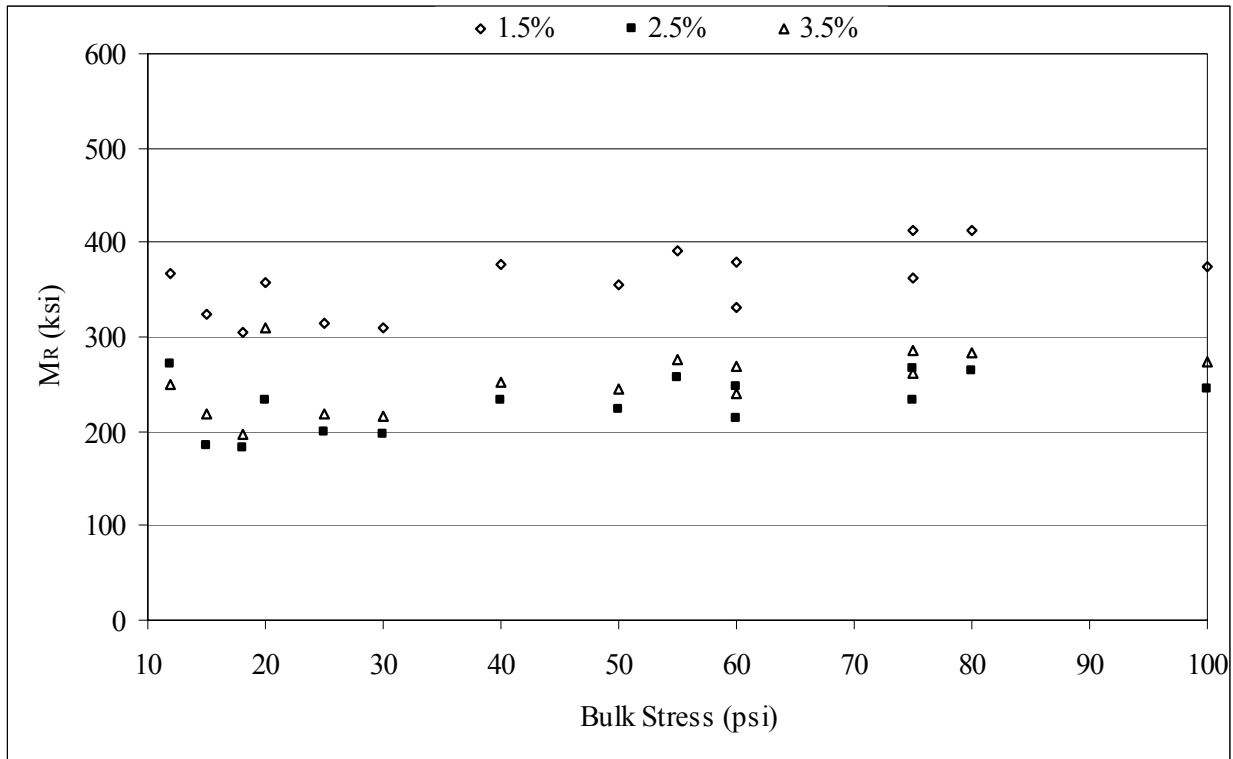
Figure 4.6 Effects of Binder Content on M_R of EATB

(Northern Region, 20°C)

Compare to binder content, aggregate source has more significant influence on modulus of EATB. As shown in Figure 4.7, Central region EATB had the highest M_R value among materials from three regions, which was as twice as M_R value of materials obtain from Northern region.
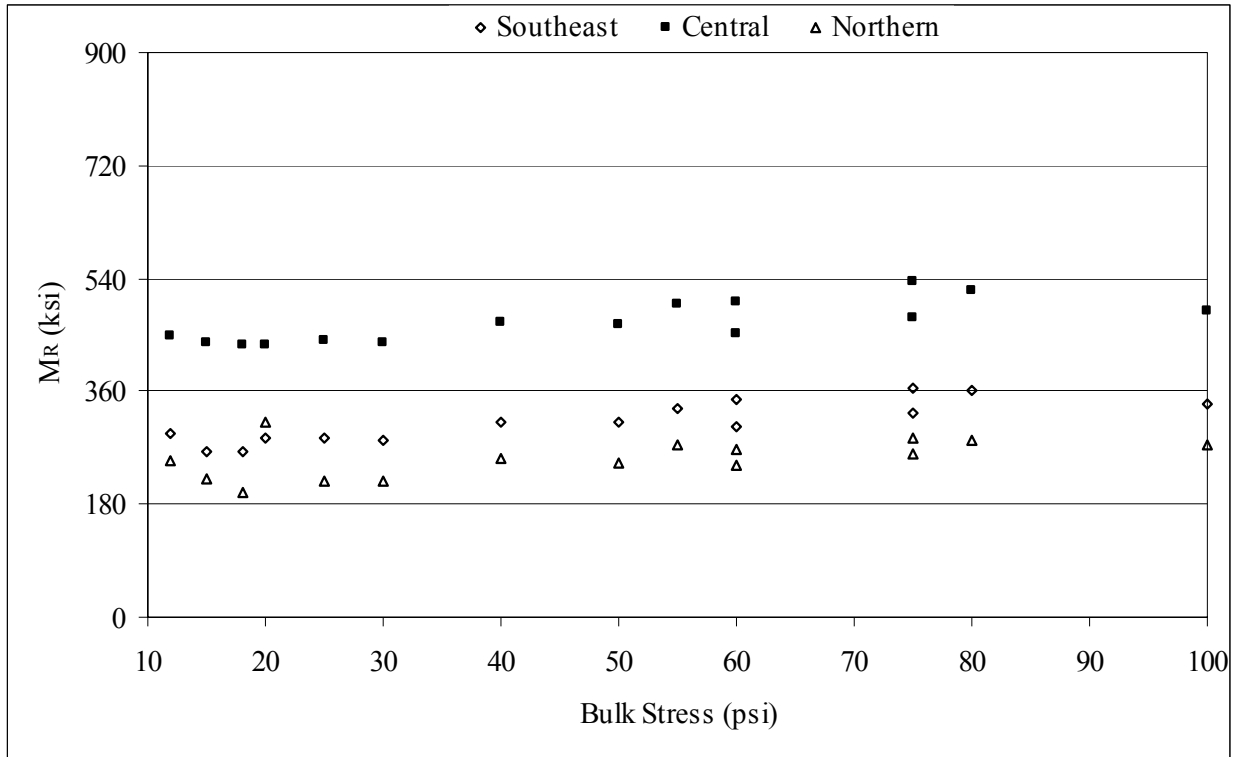
Figure 4.7 Effects of Temperature on M_R of EATB

(20^oC, 3.5% Residual Binder)

For EATB, Equations 4.3 shows the effects of binder content, temperature, and aggregate properties on (k_1). The analysis did not show statistically significant influences (at the 95% confidence level) of binder content, temperature, or aggregate source on the regression constant k_2 and k_3. An prediction model for M_R of FATB was developed, as shown in Equation 4.3. The overall R^2 equals to 82%.

$$M_R = e^{4.1205+0.0025\,F-0.0567\,T-0.0048\,P_b} P_a \left(\frac{\theta}{P_a} \right)^{0.0842} \left(\frac{\tau_{oct}}{P_a} + 1 \right)^{-0.2236} \qquad R^2 = 82\% \qquad (4.3)$$

where,

M_R = resilient modulus, ksi,

θ = bulk stress, $\sigma_1+\sigma_2+\sigma_3$, psi,

τ_{oct} = deviatoric stress, $1/3[(\sigma_1-\sigma_2)^2+(\sigma_1-\sigma_3)^2+(\sigma_2-\sigma_3)^2]^{1/2}$, psi,

P_a = atmosphere air pressure, psi, and

k_1, k_2, k_3 = regression constants.

F = fractured surface, %

T = temperature, °C, and

P_b = percent binder by total weight, %.

Foamed asphalt treated base

M_R of FATB is also affected by temperature. Generally, as temperature decreased, the M_R increased (Figure.4.8). The value of M_R was doubled when temperature dropped from 20°C to -10°C. However, compared to HATB and EATB, this effect was less significant. During foaming and mixing process, asphalt was dispersed into small droplets between mineral particles. These droplets improved the connection between these particles. At low temperature, stiffness increased at the points where mineral particles bounded by asphalt droplets. Without asphalt, the connection between particles did not change much when temperature dropped. This explained that why FATB is less sensitive to the change of temperature than HATB and EATB.

For Northern region at 20°C (Figure 4.9), the M_R of FATB at 2.5% residual binder content was slightly higher than that at 1.5% binder content; FATB with 3.5% binder content had the lowest M_R. This was consistent with the finding from Nataatmadja's study (2001), in which for the specimens prepared with the Marshall compactor with binder content ranging from 1.5% to 4.25%, there was an optimum binder content of 2.2% corresponding to the highest stiffness. Other studies (Muthen 1998, Kim and Lee 2006) also showed a similar trend. In FATBs, the fines and the foamed asphalt together produce a mortar, binding the coarse aggregates. The fines content is a critical factor to determine the binder content of FATBs with highest stiffness (Wirtgen 2002). The fines content of D-1 materials in this study is 3.15%,
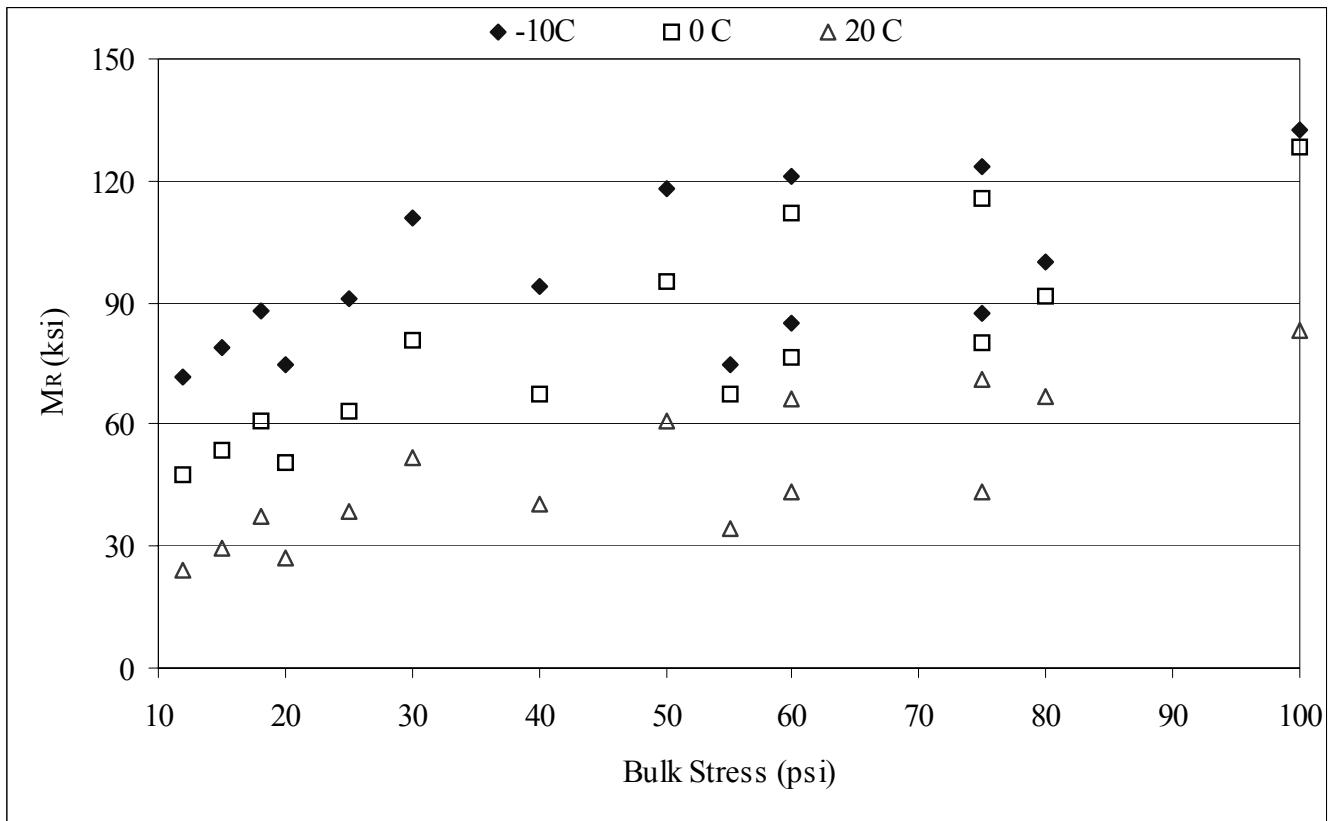
Figure 4.8 Effects of Temperature on M_R of FATB
(Northern region, 3.5% binder)

which was much lower than the common field practice for FATB with up to 20% fines content (Eller and Olson 2009). In this study, at higher binder content of 3.5%, more fines would be required for foamed asphalt to mobilize its bounding effects. The mortar composed of lower fines content (3.15%) and higher binder content (3.5%) may act more like a lubricant, reducing the internal friction of the aggregate skeleton, leading to an M_R decrease. This may account for the lower modulus obtained at 3.5% binder content. On the other hand, at lower binder content (1.5% in this study), lower binder content would not provide enough binding strength to hold particles together and, therefore, result in lower modulus.
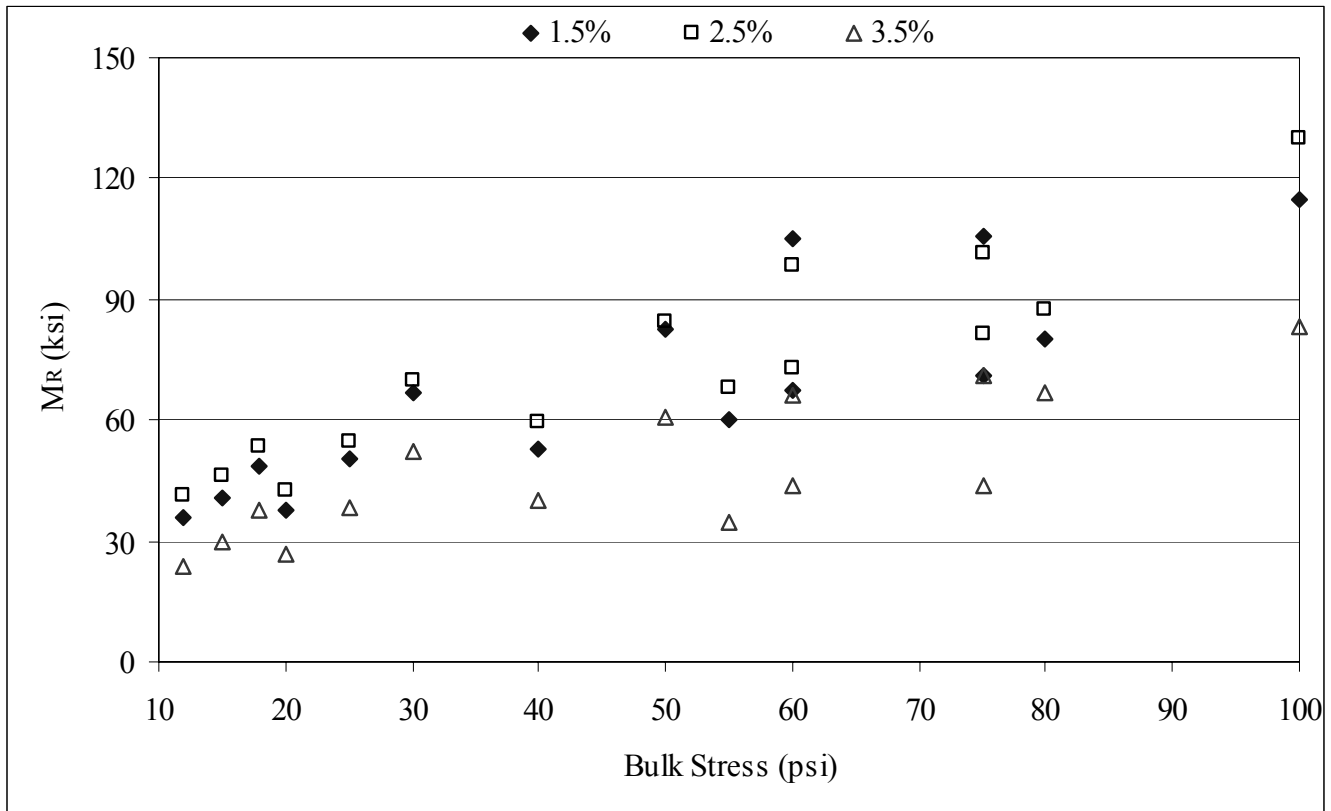
Figure 4.9 Effects of Binder Content on M_R of FATB

(Northern region, 20^oC)

As shown in Figure 4.10, the effect of aggregate was more significant for lightly bound material such as FATB. D-1 material from the Northern region was least angular, while D-1 materials from the Southeast and Central regions had better angularities. Shape and surface texture have great influence on the performance of asphalt-treated materials (Kandhal and Parker 1998, Prowell et al. 2005) where aggregates are relied upon to provide stiffness and strength by interlocking with one another. Better angularity improved the interlock between aggregate particles, which improved the overall shear resistance of the ATB specimens, leading to higher M_R. The effect of aggregate was more significant for lightly bound material such as FATB. The M_R of FATB made with the least angular D-1 material from the Northern region was only about 50% of that from the Southeast region, as shown in Figure 4.10.
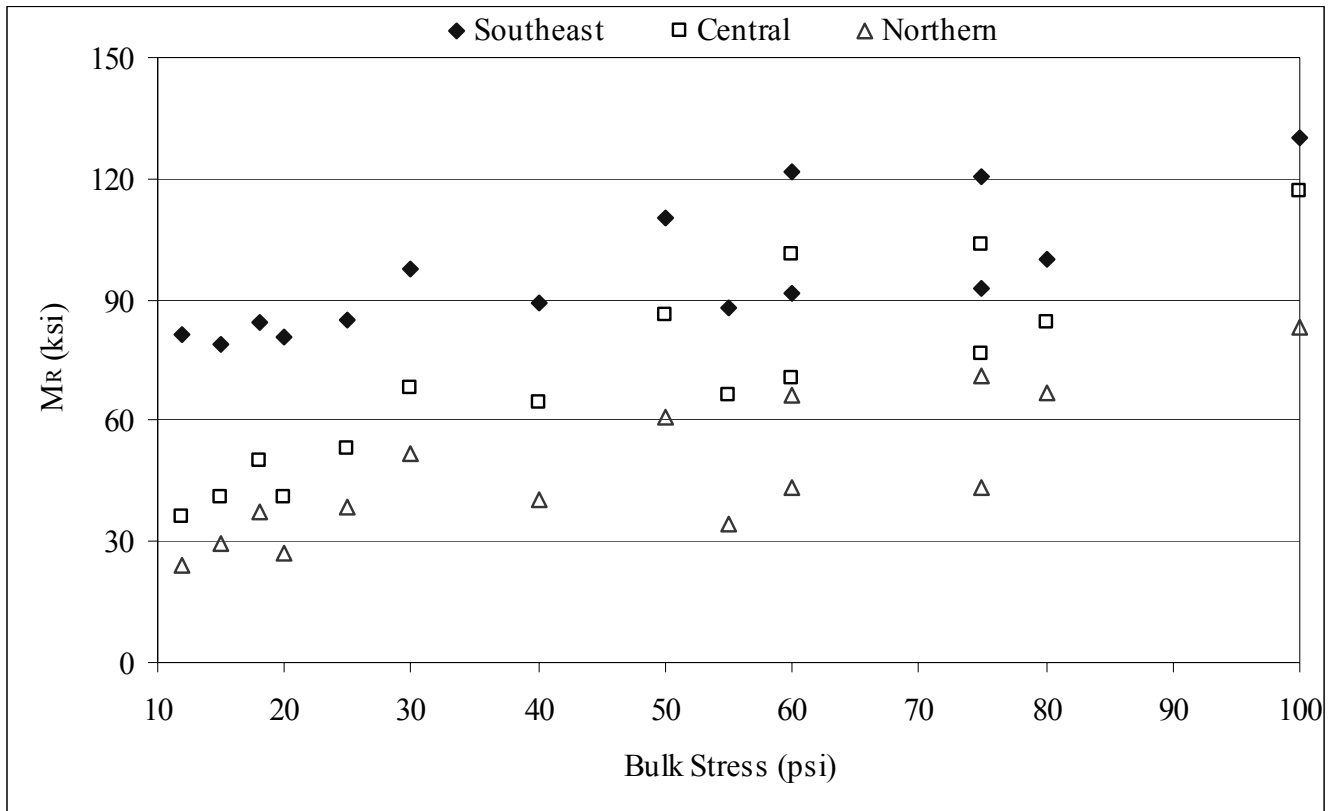
Figure 4.10 Effects of Aggregate Resource on M_R of FATB

(3.5% binder content, 20$^{\text{o}}$C)

Without exception, the M_R of FATB also exhibited the stress dependent behavior. As indicated in Figure 4.11, at each confining pressure level, the M_R of FATB increased greatly with the increase of deviator stress. However, under same deviator stress, the increase of M_R with the increase of confining pressure was insignificant. Therefore, compare to HATB and EATB, amplitudes of deviator stress played a more important role for FATBs.
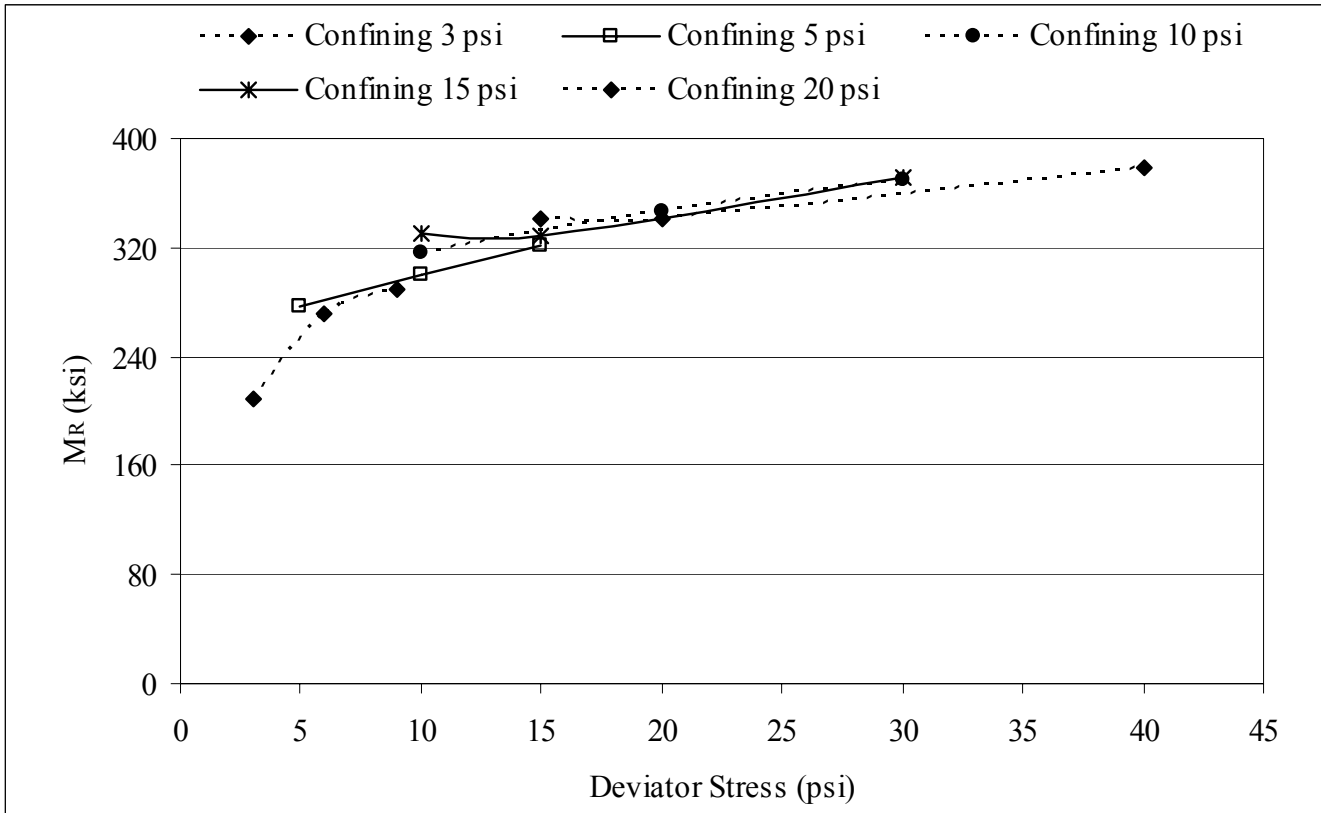
Figure 4.11 Effects of Stress State on M_R of FATB

(2.5% Binder, Southern Region, 0°C)

For FATB, statistical analysis showed binder content, temperature, and aggregate properties affected the values of k_1 and k_3, but did not have a significant effect on k_2. An overall expression for M_R of FATB was developed, as shown in Equation 4.4.

$$M_R = e^{-2.9060+0.0623F-0.0363T-0.2346P_b} P_a \left(\frac{\theta}{P_a}\right)^{0.0029} \left(\frac{\tau_{oct}}{P_a}+1\right)^{4.2850-0.0434F+0.0206T+0.1365P_b} \qquad R^2=80\% \qquad (4.4)$$

where,

M_R = resilient modulus, ksi,

θ = bulk stress, $\sigma_1+\sigma_2+\sigma_3$, psi,

τ_{oct} = deviator stress, $1/3[(\sigma_1-\sigma_2)^2+(\sigma_1-\sigma_3)^2+(\sigma_2-\sigma_3)^2]^{1/2}$, psi,

P_a = atmosphere air pressure, psi, and

k_1, k_2, k_3 = regression constants.

F   = fractured surface, %

T   = temperature, °C, and

P_b = percent binder by total weight, %.

D-1 Blended with RAP at 50% to 50% Ratio

Triaxial tests were also performed on a mixture of RAP and D-1 material at 50%:50% ratio. Stabilization agent was not added to this material. The tests were performed at the optimum water content at three different temperatures. Because $0°C$ is the critical temperature for water, a little temperature variance from $0°C$ will cause great changes on behavior of water. These changes will further affect the stiffness of RAP (50:50) specimens causing great variance of test result. Therefore, to avoid this happen, triaxial tests were performed at $-10°C$, $-2°C$ and $20°C$. As shown in Figure 4.12, M_R of RAP (50:50) increased almost 20 times higher when temperature dropped to $-10°C$ from $20 °C$. Because RAP occupied 50% of overall component in each sample, the effect of aggregate source was not obvious as on ATBs. At $20°C$, M_R of RAP (50:50) presented a great stress state dependent property. As confining pressure increased form 3 psi to 20 psi, the moduli increased 2 times. Increment of deviator stress also leads to the increase of M_R.
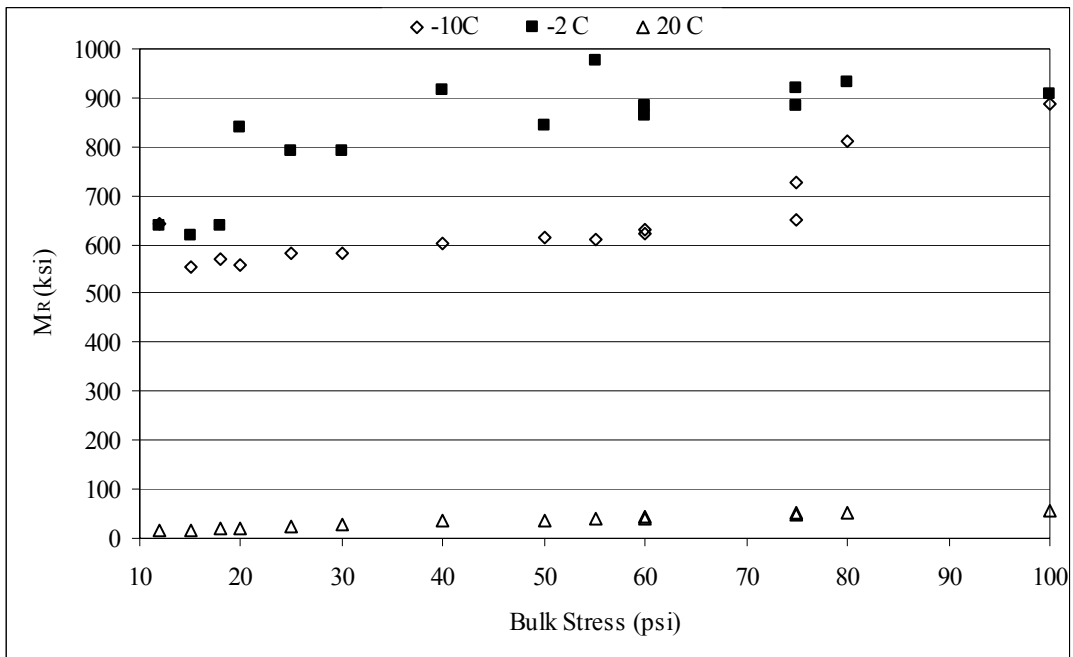
Figure 4.12 Effects of Temperature on M_R of RAP (50:50)

(Northern Region)
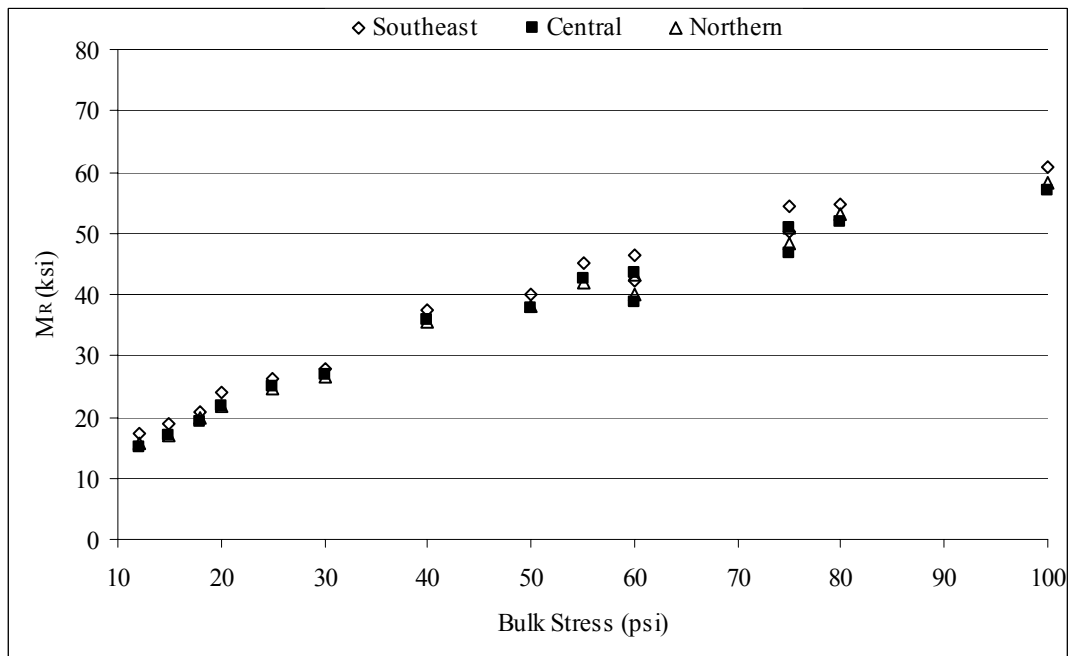
Figure 4.13 Effects of Aggregate Source on M_R of RAP (50:50)

$(20^o C)$
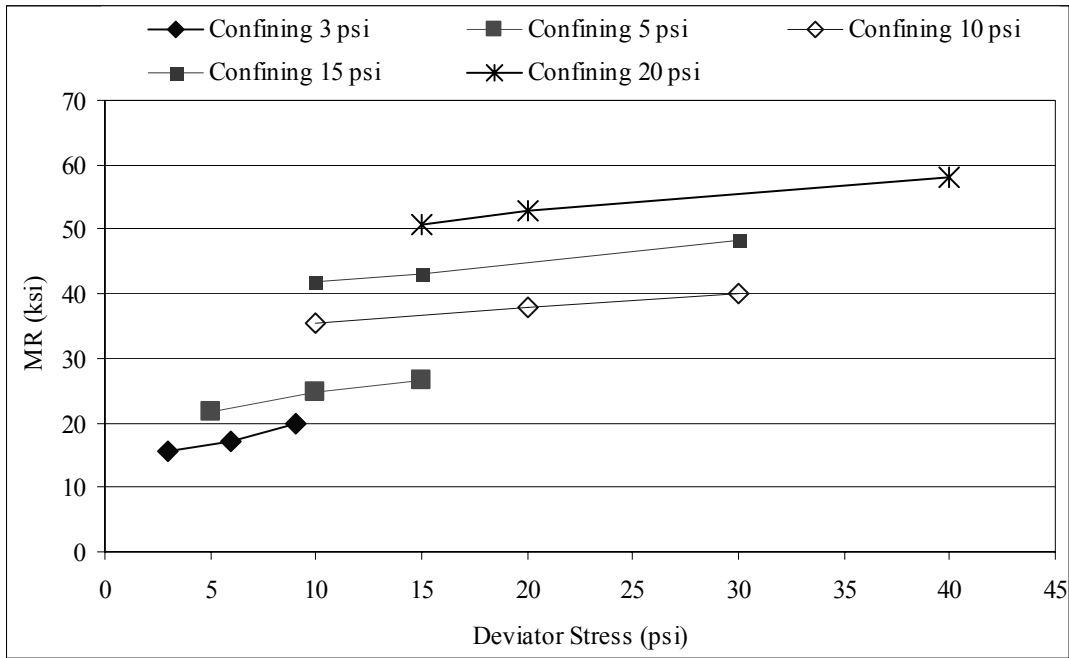
Figure 4.14 Effects of Stress State on M_R of RAP (50:50)

(Northern Region, 20°C)

A predicting model was developed for mixture of RAP and D-1 material at 50% to 50% ratio. The statistical analysis indicated that percentage of fractured surface and testing temperature had effects on all three regression constants, k_1, k_2 and k_3. The final model has been proposed as Equation 4.5.

$$M_R = e^{-9.0482+0.1294F-0.1660T} P_a \left(\frac{\theta}{P_a}\right)^{4.5056-0.00406F+0.0586T} \left(\frac{\tau_{oct}}{P_a}+1\right)^{0.15781-0.0099F-0.031T} \qquad R^2 = 87\% \quad (4.5)$$

where,

M_R = resilient modulus, ksi,

θ = bulk stress, $\sigma_1+\sigma_2+\sigma_3$, psi,

τ_{oct} = deviatoric stress, $1/3[(\sigma_1-\sigma_2)^2+(\sigma_1-\sigma_3)^2+(\sigma_2-\sigma_3)^2]^{1/2}$, psi,

P_a = atmosphere air pressure, psi, and

F   =   fractured surface, %

T   =   temperature, °C, and

RUTTING TEST

Figures 4.15−4.17 illustrate rutting results of HATBs from all three regions. Generally, the performance of rutting resistance of Southeast material was better than those from the Central and Northern regions. The rutting depth increased dramatically at the first 1000 loading cycles, roughly accounting for 50% of total rutting depth. At 3.5% binder content, HATB specimens had the best rutting resistance. For materials from Southeast and Central regions, the highest rutting depth was observed at 4.5% binder content and, for materials from Northern region, HATB with 2.5% binder content had highest rutting depth. Because of the great rutting depth, the tests even could not be completed in these worst conditions.
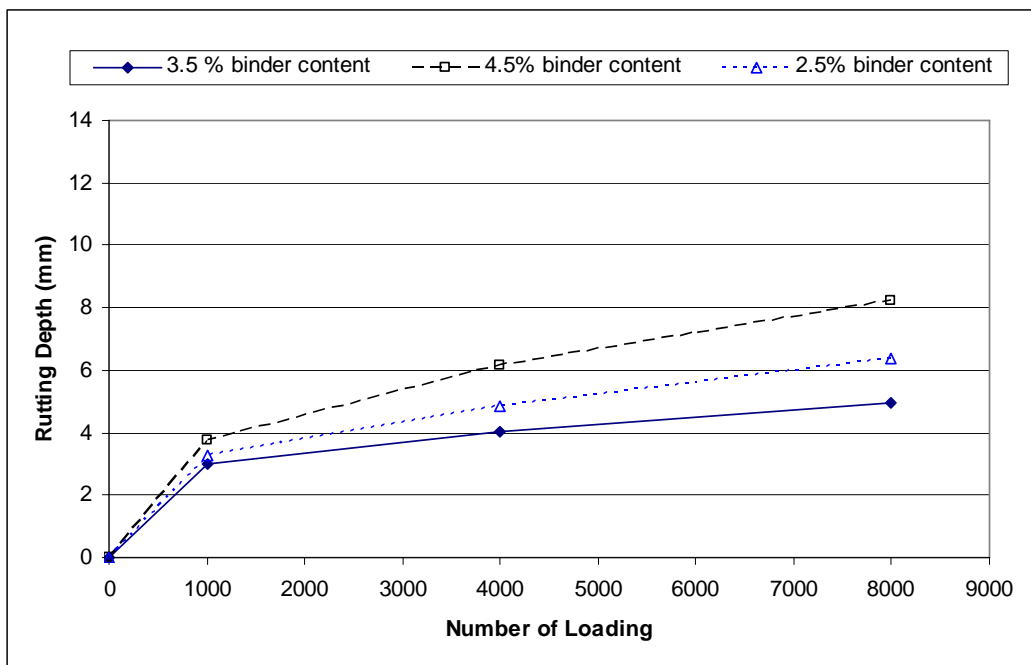
Figure 4.15 Rutting Depth of HATB for Southeast Region
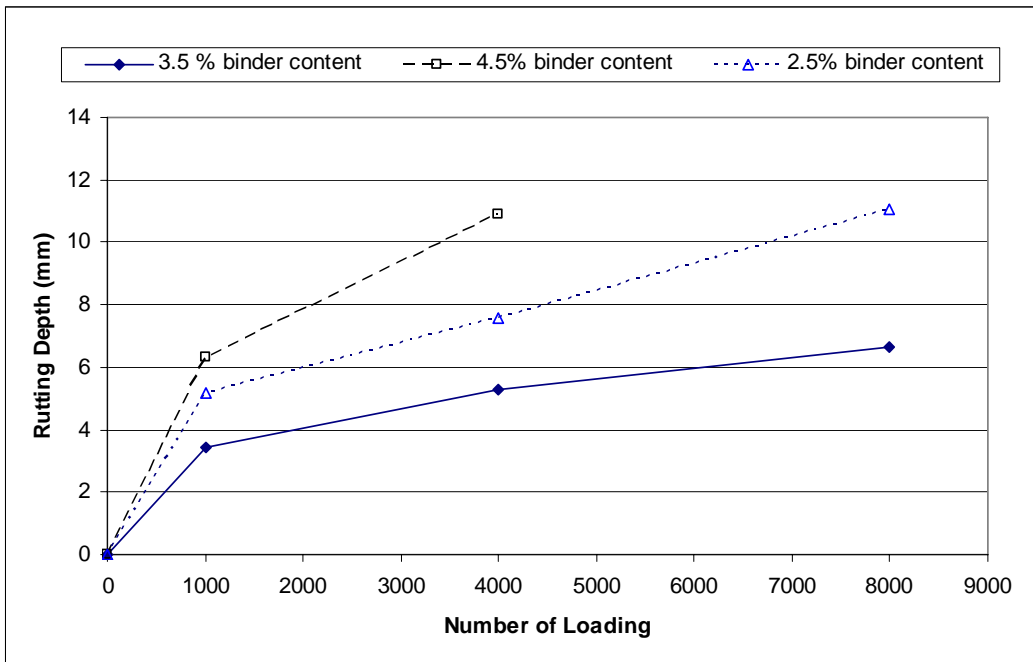
Figure 4.16 Rutting Depth of HATB for Central Region
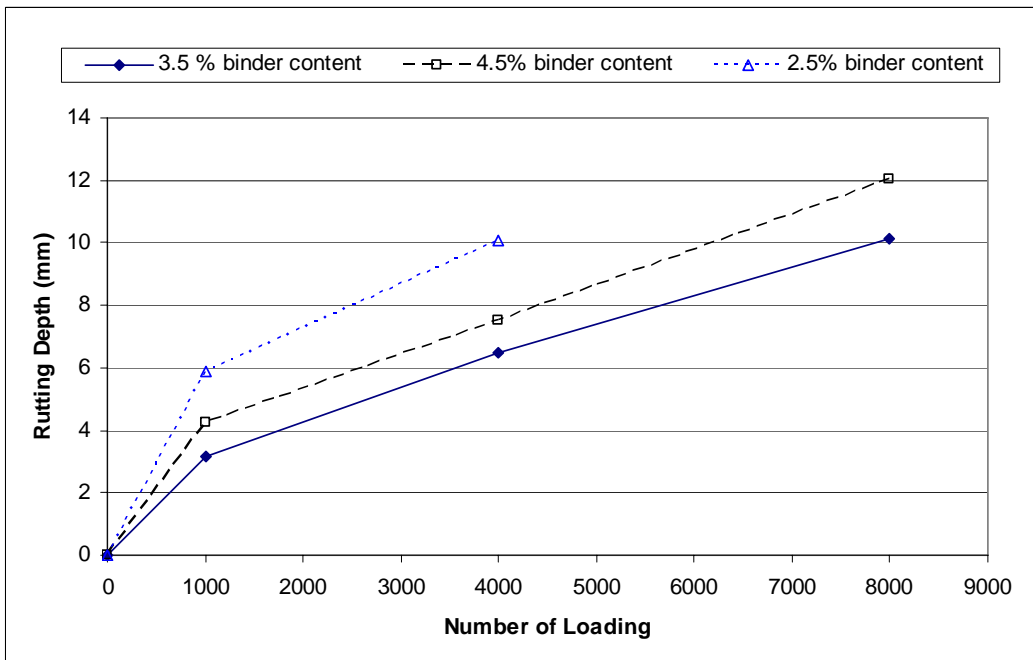
Figure 4.17 Rutting Depth of HATB for Northern Region

FATIGUE TEST

The fatigue tests were performed on HATB specimens with materials form Northern, Central and Southeast regions. Two binder contents (3.5% and 4.5%) were used for each region. The fatigue tests were conducted at $20^{o}C$ under strain-control mode, which means during the entire test process, the beam specimen was controlled to be bent at constant strain. Three strain levels were applied to investigate the effects of loading amplitude on fatigue performance of HATB. Tables 4.2−4.4 list the fatigue testing results of HATBs. With the increase of loading amplitude, the bending repetition decreased dramatically. Specimens with 4.5% binder content showed higher fatigue life than those with 3.5% binder content. It means higher binder content increased the fatigue resistance of HATB. The results are also illustrated in figure 4.18−4.20 that, fatigue life of each specimen and loading strain level represents a linear relationship. The regression analysis showed the R^2s of both HATB with 3.5% and 4.5% binder contents were higher than 95%. Trial testing for HATB with 2.5% binder was also performed. However, due to the extremely low binder content, beam specimens collapsed during the cutting process and results of fatigue tests at 2.5% binder content were not available.

Table 4.2 Beam Fatigue Test Result of Northern Region HATB

Binder Content	Micro-strain	Repetition	Binder Content	micro-strain	Repetition
3.5%	300	567200	4.5%	200	2976850
	300	267852		400	185050
	400	69200		400	122900
	500	8000		500	68700
	500	20650		500	75400

Table 4.3 Beam Fatigue Test Result of Central Region HATB

Binder Content	Micro-strain	Repetition	Binder Content	micro-strain	Repetition
3.5%	300	120500	4.5%	300	466850
	300	127800		300	468800
	400	63450		400	179150
	400	32450		400	245250
	500	23700		500	59650
	500	35650		500	100000

Table 4.4 Beam Fatigue Test Result of Southeast Region HATB

Binder Content	Micro-strain	Repetition	Binder Content	micro-strain	Repetition
3.5%	300	132100	4.5%	300	637750
	300	59100		300	493850
	400	-		400	310500
	400	33349		400	93050
	500	22850		500	56750
	500	14650		500	56650
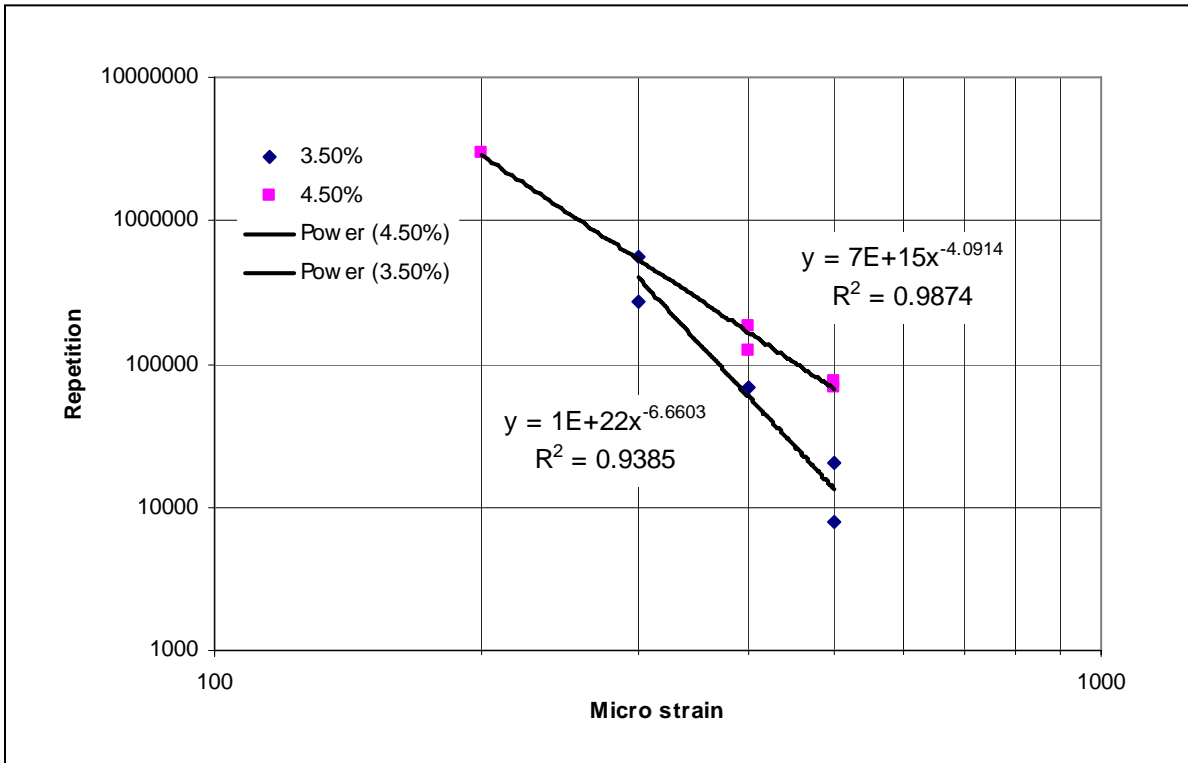
Figure 4.18 Beam Fatigue Test Result (Northern region)
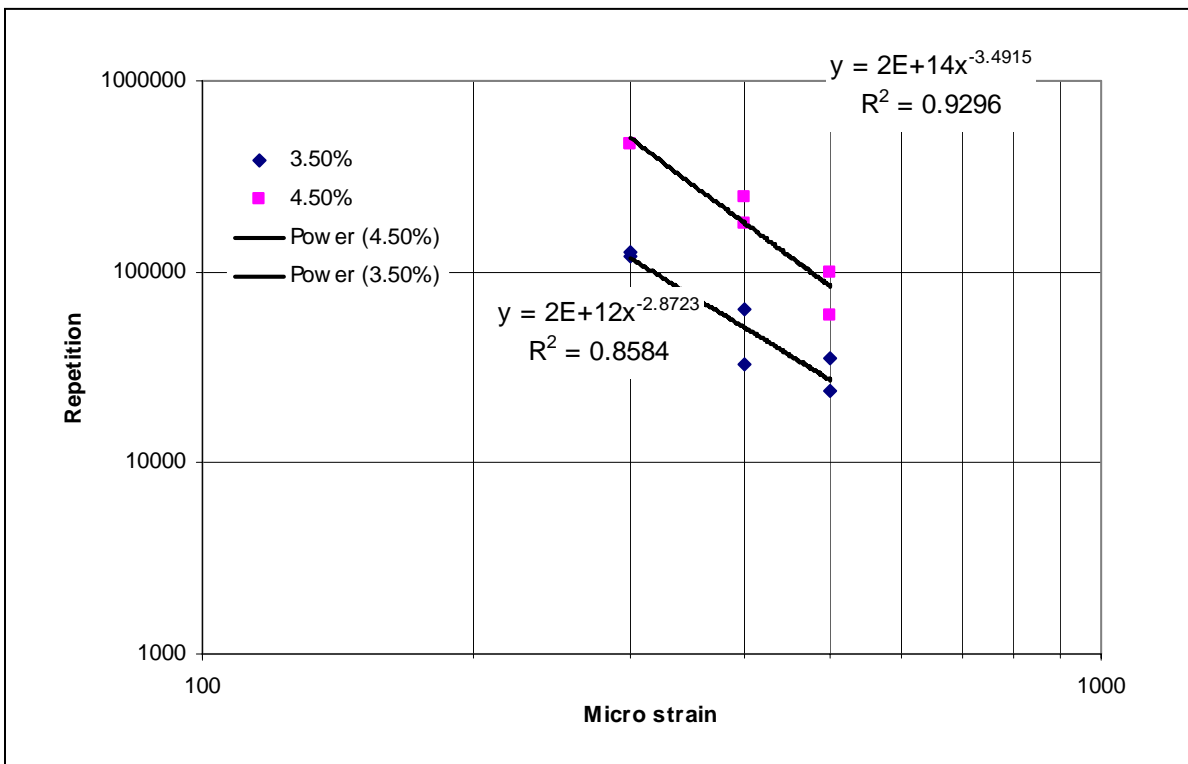
Figure 4.19 Beam Fatigue Test Result (Central Region)
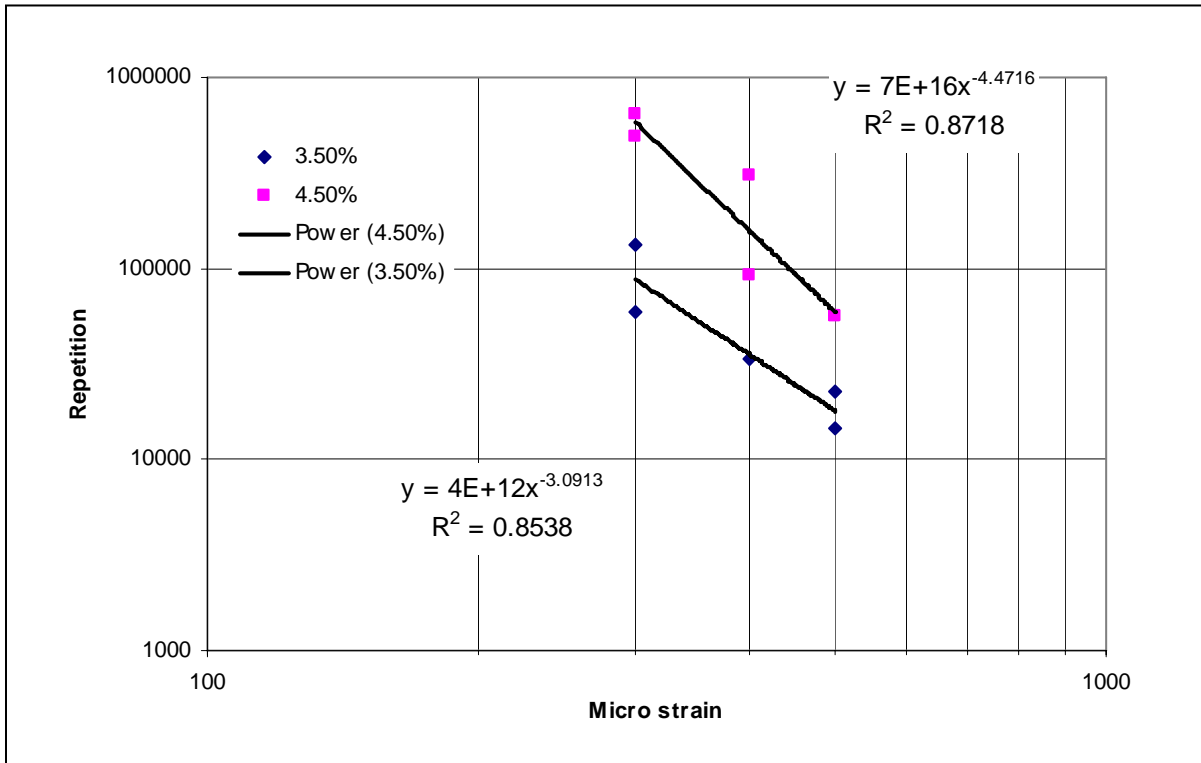
Figure 4.20 Beam Fatigue Test Result (Southeast Region)

CHAPTER V

CONLUSIONS AND RECOMMENDATIONS

CONCLUSIONS

Based on the literature review and laboratory tests conducted in this study, the conclusions can be drawn that:

1. Asphalt treatment effectively increases M_R the of D-1 material. Among three treatment techniques, hot asphalt treatment has the most significant improvement, followed by emulsified asphalt treatment and foamed asphalt treatment. Blending D-1 material with RAP is also considered as a treatment techniques, because there till a mount of asphalt cement remained on the individual particles r of RAP. However, this expected improvement may need long time after construction to be fulfilled. In this study, the 50:50 RPA specimens was tested right after the fabrication, and no obvious improvement on the M_R has been observed.

2. The M_Rs of HATB, EATB, FATB and 50:50 RAP exhibited stress-state dependent properties. Generally, the M_Rs increased with the increase of confining pressure (σ_3) and deviator stress (σ_d). This dependency varies for different types of material.

3. As expected, the M_Rs of ATBs increased with a decrease in temperature. FATB has the lowest temperature sensitivity.

4. Using higher binder content for treatment does not increase the M_R of ATBs. In this study, it has been observed that, generally, low binder content produced higher moduli. However, this doesn't mean that ATBs with lower binder content have better performance when paved on the roadways. In the layered pavement structure, materials with higher M_R helps reducing the stresses in the

72

upper and lower layers, meanwhile it will increase the stress in the layer where they are paved. In addition, lower binder content lead to less flexibility, which means lower fatigue resistance for asphalt mixture. The selection of asphalt binder content should not only depends on the improvement of moduli, but also include the consideration of durability and structure design.

5. Aggregate source affects the M_R of ATBs. Northern region ATBs had the lowest M_R among three regions of Alaska due to least-angular D-1 material. However, the effect of aggregate properties on 50:50 RAP is not significant.

6. Predicting equations for M_R were developed based on the current stress-dependent AASHTO MEPDG model. The effects of temperature and material variables have been also integrated into the models. The equations obtained through this study are as follows:

$$M_R = e^{1.1548+0.04736F-0.0596T-0.1723P_b} P_a \left(\frac{\theta}{P_a}\right)^{0.2669} \left(\frac{\tau_{oct}}{P_a}+1\right)^{-0.4109} \quad \text{(HATB)}$$

$$M_R = e^{4.1205+0.0025F-0.0567T-0.0048P_b} P_a \left(\frac{\theta}{P_a}\right)^{0.0842} \left(\frac{\tau_{oct}}{P_a}+1\right)^{-0.2236} \quad \text{(EATB)}$$

$$M_R = e^{-2.9060+0.0623F-0.0363T-0.2346P_b} P_a \left(\frac{\theta}{P_a}\right)^{0.0029} \left(\frac{\tau_{oct}}{P_a}+1\right)^{4.2850-0.0434F+0.0206T+0.1365P_b} \quad \text{(FATB)}$$

$$M_R = e^{-9.0482+0.1294F-0.1660T} P_a \left(\frac{\theta}{P_a}\right)^{4.5056-0.00406F+0.0586T} \left(\frac{\tau_{oct}}{P_a}+1\right)^{0.15781-0.0099F-0.031T} \quad \text{(50:50 RAP)}$$

where,

M_R = resilient modulus, ksi,

θ = bulk stress, $\sigma_1+\sigma_2+\sigma_3$, psi,

τ_{oct} = deviatoric stress, $1/3[(\sigma_1-\sigma_2)^2+(\sigma_1-\sigma_3)^2+(\sigma_2-\sigma_3)^2]^{1/2}$, psi,

P_a = atmosphere air pressure, psi, and

k_1, k_2, k_3 = regression constants.

F = fractured surface, %

T   = temperature, °C, and

P_b = percent binder by total weight, %.

7. Due to the material properties, rutting test were only performed on HATBs. HATB produced with D-1 materials southeast has the best rut resistance and the northern region has the lowest. For three regions, HATB with 3.5% binder content has the best rutting resistance.

8. Increase the binder content will increase the fatigue resistance of HATB based on the test results on specimens with 3.5% and 4.5% binder content. Due to the extremely low binder content, specimens with 2.5% binder content collapsed before testing.

RECOMMENDATIONS

Based on the predicting equations for M_R, moduli of treated base course material can be calculated according to treatment technique, ambient temperature, aggregate properties, and binder content. Future study is needed to further validate these predicting equations. This should be accomplished by applying case studies of pavement designs with different materials inputs based on these predicting equations in AKFPD and MEPDG programs. Data from field ATB projects regarding materials inputs and pavement performance will be also needed to compare with those based on predicting equations and pavement design programs.

REFERENCE

American Association of State Highway & Transportation Officials. (1993) *Guide for Design of Pavement Structures.* Washington, DC.

Anderson, J. R., and Thompson, M. R. (1995). "Characterization of Emulsion Aggregate Mixtures." *Transportation Research Board 1942*, Transportation Research Board, Washington, D.C., 108−117.

ARA, Inc. (2000). "Guide for Mechanistic−Empirical Design of New and Rehabilitated Pavement Structures, Appendix DD−1: Resilient Modulus as Function of Soil Moisture−Summary of Predictive Models." *NCHRP Report No. A-37A,* Transportation Research Board, Washington, D.C.

Aschenbrener, T. (1995). "Evaluation of Hamburg Wheel-Tracking Device to Predict Moisture Damage in Hot Mix Asphalt." *Transportation Research Record 1492,* National Research Council, Washington, D.C., 193-201.

Asi, I. M. (2001). "Stabilization of Sebkha Soil Using Foamed Asphalt." *Journal of Materials in Civil Engineering,* 13(5), 324−340.

ASTM (1995) "Standard Test Method for Indirect Tensile (IDT) Strength of Bituminous Mixtures." *D-4123*. ASTM International, West Conshohocken, PA.

ASTM. (2007). "Standard Test Methods for Laboratory Compaction Characteristics of Soil Using Modified Effort." *D−1557*. ASTM International, West Conshohocken, PA.

Barksdale, R. D. (1971). "Compressive Stress Pulse Times in Flexible Pavements for Use in Dynamic Testing." *Highway Research Board 345*, Highway Research Board, Washington, D.C., 32−44.

Barksdale, R. D., Alba, J., Khosla, N.P., Kim, R., Lambe, P. C., and Rahman, M. S. (1997). "Laboratory Determination of Resilient Modulus for Flexible Pavement Design. Final Report." *NCHRP Report No. 1-28,* Transportation Research Board, Washington, D.C.

Bazin, P., and Saunier, J., (1967). "Deformability, Fatigue and Healing Properties of Asphalt Mixes." *Proceedings, International Conference on the Structural Design of Asphalt Pavements*, , University of Michigan, Ann Arbor.

Bissada, A.F. (1987). "Structural Response of Foamed –Asphalt-sand Mixtures in Hot Environments." *Transportation Research Record 1115*, Transportation Research Board, Washington, D.C., 134−149.

Brown, E. R., Kandhal, P. S., Roberts, F. L., Kim, Y. R., Lee, D., and Kennedy, T. W. (2009). *Hot Mix Asphalt Materials, Mixture Design, and Construction*. Third Edition, NAPA Research and Education Foundation, Lanham, Maryland.

Brown, S. F. (1973). "Determination of Young's Modulus for bituminous Materials in Pavement Design." *Highway Research Board 431*, Highway Research Board, Washington, D.C., 38−49.

Collins, R., Watson, D., and Campbell, B. (1995). "Development and Use of the Georgia Loaded Wheel Tester." *Transportation Research Record 1492,* Transportation Research Board, Washington, DC., 202–207

Collins, R., Shami, H., and Lai, J.S. (1996). "Use of Georgia Loaded Wheel Tester to Evaluate Rutting of Asphalt Samples Prepared by Superpave Gyratory Compactor." *Transportation Research Record 1545,* Transportation Research Board, Washington, DC., 161–168.

Deacon, J., Tayebali, A., Coplantz, J., Finn, F., and Monismith, C. (1994) "Fatigue Response of Asphalt-Aggregate Mixes." *SHRP-A-404*, National Research Council, Washington, D.C.

Eller A., and Olson, R. (2009). "Recycled Pavements Using Foamed Asphalt in Minnesota." *MN/RC 2009-09, Minnesota Department of Transportation*, Maplewood, MN

Epps, J.A., and Monismith, C.L. (1972). "Fatigue of Asphalt Concrete Mixtures -Summary of Existing Information", *STP 508*, ASTM, 19-45.

Farrar, M. J., and Ksaibati, K. (1996). "Resilient Modulus Testing of Lean Emulsified Asphalt." *Transportation Research Record 1546*, Transportation Research Board, Washington, D.C., 32−40.

Fu, P., and Harvey, J. T. (2007). "Temperature Sensitivity of Foamed Asphalt Mix Stiffness: Field and Lab Study." *International Journal of Pavement Engineering,* 8(2), 137−145.

Gartin, R. S., and Esch, D. C. (1991). "Treated Base Course Performance in Alaska", *Alaska Department of Transportation and Public Facilities*, Juneau, AK.

Green, J. G. (2004). "Standard Specifications for Highway Construction." *Alaska Department of Transportation and Public Facilities*. Juneau, AK.

Hanson, D.I., and Cooley, Jr. L.A., (1999). "Study to Improve Asphalt Mixes in South Carolina, Vol. III: Modified Mixes." *Report No. FHWA-SC-98-02*, FHWA, USDOT, Washington, DC.

Heukelom, W., and Klomp, A.J.G. (1962), "Dynamic testing as a means of controlling pavement during and after construction," *Proceedings of the 1st international conference on the structural design of asphalt pavement,* University of Michigan, Ann Arbor, MI. "

Hicks, R. G., and Monismith, C. L. (1971). "Factors Influencing the Resilient Response of Granular Materials." *Highway Research Board 345*, Highway Research Board, Washington, D.C., 15−31.

Hittle, J.E. and Goetz, W.H., (1947) "A Cyclic Load Test Procedure." Spec.Tech. Pub. No. 79, ASTM, 72-82.

Hodek, R.J. (2007) "Resilient Modulus at the Limits of Gradation and Varying Degrees of Saturation" *Report RC-1497*, Michigan Department of Transportation, Lansing, MI

Hossain, M., Chowdhury, T., Chitrapu, S., and Gisi, A.J. (2000) "Network-Level Pavement Deflection Testing and Structural Evaluation." *Journal of Testing and Evaluation,* Vol. 28, 199-206.

Huang, Y. H. (2004). *Pavement analysis and design*. Pearson Education, Inc., Upper Saddle River, NJ.

Jenkins, K. J., Long, F. M., and Ebels, L. J. (2007). "Foamed Bitumen Mixes = Shear Performance?" *International Journal of Pavement Engineering*, 8(2), 85–98.

Kalcheff, I. V., and Hicks, R.G. (1973). "A Test Procedure for Determining the Resilient Properties of Granular Material." *Journal of Testing and Evaluation,* 1(6), 427−479.

Kandhal, P. S. and Cooley, L. A. (2003). "Accelerated laboratory Rutting Tests: Evaluation of the Asphalt Pavement Analyzer." *NCHRP Report 508*, Transportation Research Board, Washington, DC.

Kandhal, P.S., and Parker, F. Jr. (1998). "Aggregate Tests Related to Asphalt Concrete Performance in Pavements." *NCHRP Report 405*, Transportation Research Board, Washington, DC.

Kandhal, P.S., and Mallick, R.B., (1999) "Evaluation of Asphalt Pavement Analyzer for HMA Mix Design." *NCAT Report 99-4,* National Center for Asphalt Technology, Auburn, AL.

Kennedy , W.H. and Hudson, W.R. (1968) " Application of Indirect Tensile Test to Stabilized Materials." Annual Highway Research Board Meeting, 1968.

Kim, W., Labuz, J. F. and Dai, S. (2007). "Resilient Modulus of Base Course Containing Recycled Asphalt Pavement", *Transportation Research Board 2006*, Transportation Research Board, Washington, D.C., 27-35.

Kim, Y., and Lee, H. (2006). "Development of Mix Design Procedure for Cold In−Place Recycling with Foamed Asphalt." *Journal of Materials in Civil Engineering*, 18(1), 116−124.

Kim, Y., Lee, H., and Heitzman, M. (2007). "Validation of New Mix Design Procedure for Cold In−Place Recycling with Foamed Asphalt." *Journal of Materials in Civil Engineering,* 19(11), 1000−1010.

Kirk, J. M. (1967). "Results of Atigue Tests on Different Types of Bituminous Mixtures," *Proceedings, International Conference on the Structural Design of Asphalt P*av*ements*, University of Michigan, Ann Arbor, MI.

Lai, J.S. (1988). "Evaluation of the Effect of Gradation of Aggregate on Rutting Characteristics of Asphalt Mixes." *Project No. 8706*, Georgia DOT.

Li, P., Liu, J. and Saboundjian, S. (2009). "Resilient Modulus Characterization of Hot Asphalt Treated Alaskan Base Course Material." *ASCE Geotechnical Special Publication No. 191*, 168–176.

Loizos A., and Plat, C., (2007). "Ground Penetrating Radar as an Engineering Diagnostic Tool for Foamed Asphalt Treated Pavement Layers." *International Journal of Pavement Engineering,* 8(2), 147–155.

Loizos, A. (2007). "In−Situ Characterization of Foamed Bitumen Treated Layer Mixes for Heavy−Duty Pavements." *International Journal of Pavement Engineering,* 8(2), 123–135.

Loizos, A., and Papavasiliou, V. (2006). "Evaluation of Foamed Asphalt Cold In−Place Pavement Recycling Using Nondestructive Techniques." *Journal of Transportation Engineering,* 132(12), 970−978.

Witczak, M. W., Kaloush, K., Pellinen, T., El-Basyouny, M., and Von Quintus, H., (2002) "Simple Performance Test for Superpave Mix Design" *NCHRP Report 465*, Transportation Research Board, Washington, DC.

Maupin, G. W. Jr. (1998). "Comparison of Several Asphalt Design Methods." *VTRC 98-R15*, Virginia Transportation Research Council. Charlottesville, VA.

Mchattie, R. L. (2004). "Alaska Flexible Pavement Design Manual." *Alaska Department of Transportation and Public Facilities*, Fairbanks, AK.

McLean, D. B. (1974). "Permanent Deformation Characteristics of Asphalt Concrete." Ph.D. Thesis, University of California, Berkeley.

McLeod, N.W. (1967) "The Asphalt Institute's Layer Equivalency Program", *Res. Series 15*.Asphalt Institute, College Park, MD.

Mcleod, N.W. (1947). "A Canadian Investigation of load Testing Applied to Pavement Design." *Spec. Tech. Pub7. No. 79*, ASTM, 83-127.

Monismith, C. L. (1966). "Asphalt Mixture Behavior in Repeated Flexure.*" Report No.TE 66-66*, ITIE, California Division of Highways.

Monismith, C. L., Epps, J. A., Kasianchuk, D. A., and Mclean, D. B., (1970). "Asphalt Mixture Behavior in Repeated Flexure." *Report No. TE 70-5*, Institute of Transportation and Traffic Engineering, University of California, Berkeley,

Monismith, C.L., Epps, J. A., and Finn, F.N. (1985). "Improved *A*sphalt Mix Design." *Association of Asphalt Paving Technologists*, V.54-85.

Muthen, K. M. (1998). "Foamed Asphalt Mixes Mix Design Procedure." *SABITA Ltd & CSIR Transportek*, Pretoria, South Africa.

Nataatmadja, A. (2001). "Some Characteristics of Foamed Bitumen Mixes." *Transportation Research Record 1767*, Transportation Research Board, Washington, D.C., 120−125.

Netemeyer, R. L. (1998) "Rutting Susceptibility of Bituminous Mixtures by the Georgia Loaded Wheel Tester." *Report No. RDT98-001*, Missouri Department of Transportation.

Nijboer, L.W. (1957) "Einige Betrachtungen uber das Marshallverfabren zur Untersuchung Bituminoser Massen", Strass und Autobahn.

Noureldin, S., Zhu, K., Li, S., and Harris, D. (2003). "Network Pavement Evaluation with Falling-Weight Deflectometer and Ground-Penetrating Radar." *Transportation Research Record 1860.* Transportation Research Board, Washington, DC, 90-99.

Pan,T., Tutumluer, E. and Carpenter, S.H. (2005) "Effect of Coarse Aggregate Morphology on the Resilient Modulus of Hot-Mix Asphalt." *Transportation Research Record 1929*, Transportation Research Board, Washington, D.C., 1-9.

Pell, P. S. (1973). "Characterization of Fatigue Behavior," *Structural Design of Asphalt Concrete Pavements to Prevent Fatigue Cracking.* Special Report 140, Highway Research Board, 49-64.

Pell, P. S. and Brown, S. F. (1972), "The Characteristics of Materials for the Design of Flexible Pavement Structures." *Proceedings, Third International Conference on the Structural Design of Asphalt Pavements*, London.

Pell, P.S. (1967). "Fatigue Characteristics of Bitumen and Bituminous Mixes." *Proceedings, International Conference on the Structural Design of Asphalt Pavements*, University of Michigan, Ann Arbor.

Prowell, B., Zhang J., and Brown, E.R. (2005). "Aggregate Properties and the Performance of Superpave-Designed Hot Mix Asphalt." *NCHRP Report 539, Transportation Research Board,* Washington, D.C.

Bonaquist, R.F., Christensen, D.W., and Stump, W. (2003) "Simple Performance Tester for Superpave Mix Design: First-Article Development and Evaluation." *NCHRP Report 513*, Transportation Research Board, Washington, DC.

Raithby, K. D., and Ramshaw, J. T. (1972). "Effect of Secondary Compaction on the Fatigue Performance of a Hot-Rolled Asphalt." *TRRL-LR 471*, Crowthorne, England.

Ramanujam, J. M., and Jones, J. D. (2007). "Characterization of Foamed−bitumen Stabilization." *International Journal of Pavement Engineering,* 8(2), 111–122.

Saleh, M. F. (2007). "Effect of Rheology on the Bitumen Foamability and Mechanical Properties of Foam Bitumen Stabilised Mixes." *International Journal of Pavement Engineering,* 8(2), 99–110.

Seed, H. B., Chan, C. K., and Lee, C. E. (1962). "Resilience characteristics of Subgrade Soil and Thin Relation to Fatigue Failure in Asphalt Pavement." *First International Conference on the Structural Design of Asphalt Pavements*, University of Michigan, Ann Arbor, MI.

Seed, H.B., and McNeill, R.L., (1958). "Soil Deformation under Repeated Stress Applications." *ASTM, Spec. Tech. Pub1. No. 32*, 177-197.

Seed, H.B. and Monismith, C.L., (1962) "Strength Evaluation of Paveement Structure Elements." *Processdings, International conference on Structural design of Asphalt Pavement*, University of Michigan, Ann Arbor, MI.

Seed, H.B., Chan, C.K., and Monismith, C.L., (1955). "Effects of Repeated Loading on the Strength and Deformation of Compacted Clay." *Proceedings, HRB*, Vol. 34, 541-558.

Shami, H.I., Lai, J.S., D'Angelo, J.A., and Harmon, T.P. (1997) "Development of Temperature-Effect Model for Predicting Rutting of Asphalt Mixtures Using Georgia Loaded Wheel Tester." *Transportation Research Record 1590,* Transportation Research Board, Washington, DC., 17–22.

Shu, X., and Huang, B. (2008). "Dynamic Modulus Prediction of HMA Mixtures Based on the Viscoelastic Micromechanical Model." *Journal of Materials in Civil Engineering*, 20(8).

Stuart, K.D., and Mogawer, W.S. (1997) "Effect of Compaction Method on Rutting Susceptibility Measured by Three Wheel-Tracking Devices." Paper presented at the 76th Annual Meeting of the Transportation Research Board, Washington, DC, January 12–16.

Tangella, S.C.S. R., Craus, J., Deacon, J.A., and Monismith, C.L. (1990). "Summary Report on Fatigue Response of Asphalt Mixtures." *SHRP TM-UCB-A-003A-89-3*, University of California, Berkeley, CA.

Tayebali, A., Rowe, G., and Sousa, J. (1992). "Fatigue response of asphalt-aggregate mixtures." Paper presented at the annual meeting of the Association of Asphalt Paving Technologists, Charleston, SC, February.

Terrel, R. L., and Awad, I. S. (1972). "Resilient Behavior of Asphalt Treated Base Course Material." Washington University, Seattle , WA.

Terrel, R. L.Awad, I.S. and Foss,L.R. (1974). "Techniques for Characterizing Bituminous Materials Using a Versatile Triaxial Testing System." *ASTM Special Technical Publication.* No. 561, 47−66.

White, T.D., Haddock, J.E., Hand, A.J.T., and Fang, H. (2002) "Contributions of Pavement Structural Layers to Rutting of Hot Mix Asphalt Pavements." *NCHRP Report No. 468,* Transportation Research Board, Washington, D.C.

Uzan, J. (1985). "Characterization of Granular Material." *Transportation Research Record 1022*, Transportation Research Board, Washington, D.C., 52−28.

Van Dijk, W., and Visser, W. (1977). "The Energy Approach to Fatigue for Pavement Design." *Proceedings, The Association of Asphalt P*aving *Technologists*, Vol. 46, 1.

Virginia Department of Transportation, Materials Division. (2000). *Guidelines for 1993 AASHTO Pavement Design.* Richmond, VA.

Wirtgen G. (2002). "Foamed Bitumen −The Innovative Binding Agent for Road Construction." *Wirtgen GmbH,* Windhagen, Germany.

Witczak, M. W., Bonaquist, R., Von Quintus, H., and Kaloush, K. (2000). "Specimen Geometry and Aggregate Size Effects in Uniaxial Compression and Constant Height Shear Tests." *Journal of Association of Asphalt Paving Technologists*, 69, 733−793.

Witczak, M.W. and Uzan, J. (1988). "The Universal Airport Pavement Design System, Report I of IV: Granular Material Characterization." University of Maryland, College Park, MD.

Youngguk, S., El-Haggan, O., King, M., Joon Lee, S., and Kim, R. (2007). "Air Void Models for the Dynamic Modulus, Fatigue Cracking, and Rutting of Asphalt Concrete." *Journal of Materials in Civil Engineering*, 19(10).

Zaghloul, S.M., He, Z., Vitillo, N., and Kerr, J.B. (1998) "Project Scoping Using Falling Weight Deflectometer Testing: New Jersey Experience." *Transportation Research Record 1643*. Transportation Research Board, Washington, DC, 34-43.

APPENDIX

Table 1 M_R of HATB, Northern Region (ksi)

Deviator (psi)	Confining (psi)	θ (psi)	τ_{oct} (psi)	2.5%			3.5%			4.5%		
				-10°C	0°C	20°C	-10°C	0°C	20°C	-10°C	0°C	20°C
2.7	3	12	1.2728	1724	1145	617	1694	1057	300	1800	696	194
5.4	3	15	2.5456	2016	1214	642	1840	1267	307	2112	803	205
8.1	3	18	3.8184	2509	1463	654	1954	1331	315	2306	806	214
4.5	5	20	2.1213	2515	1342	671	1965	1329	335	2172	796	206
9	5	25	4.2426	2579	1524	676	2125	1370	352	2362	872	220
13.5	5	30	6.3640	2467	1757	680	2211	1433	368	2340	954	235
9	10	40	4.2426	2467	1848	732	2373	1538	421	2315	971	241
18	10	50	8.4853	2617	1886	735	2299	1633	435	2490	1090	262
27	10	60	12.7279	2756	2047	737	2269	1701	443	2536	1174	279
9	15	55	4.2426	2683	1966	774	2486	1813	463	2476	1067	260
13.5	15	60	6.3640	2778	2023	771	2557	1845	469	2507	1127	267
27	15	75	12.7279	2940	2142	768	2597	1938	477	2613	1255	291
13.5	20	75	6.3640	3015	2176	791	2675	1982	458	2580	1184	279
18	20	80	8.4853	3084	2187	794	2749	2014	458	2580	1264	284
36	20	100	16.9706	3366	2302	797	2894	2115	510	2803	1391	315

Table 2 M_R of HATB, Central Region (ksi)

Deviator (psi)	Confining (psi)	θ (psi)	τ_{oct} (psi)	2.5%			3.5%			4.5%		
				-10°C	0°C	20°C	-10°C	0°C	20°C	-10°C	0°C	20°C
2.7	3	12	1.2728	2099	1541	338	1352	1818	448	2364	1016	646
5.4	3	15	2.5456	2613	1929	352	1862	2675	457	3423	1247	690
8.1	3	18	3.8184	2899	2277	366	2203	3547	473	3812	1366	717
4.5	5	20	2.1213	2663	1971	370	1870	2525	469	3239	1365	711
9	5	25	4.2426	2976	2364	382	2246	3777	490	4316	1459	751
13.5	5	30	6.3640	3201	2522	384	2493	3995	494	4636	1451	749
9	10	40	4.2426	3117	2480	407	2307	3807	526	4494	1544	786
18	10	50	8.4853	3079	2497	409	2609	4275	532	4995	1518	813
27	10	60	12.7279	2915	2508	410	2552	4368	537	4405	1378	824
9	15	55	4.2426	3212	2463	432	2427	3993	562	4507	1579	825
13.5	15	60	6.3640	3286	2545	437	2619	4385	565	5091	1609	856
27	15	75	12.7279	3045	2534	428	2697	4383	562	4865	1481	864
13.5	20	75	6.3640	3327	2542	450	2751	4653	594	5153	1653	880
18	20	80	8.4853	3279	2552	447	2854	4441	592	5285	1671	881
36	20	100	16.9706	3066	2545	449	2836	4519	598	4581	1483	900

Table 3 M_R of HATB, Southeast Region (ksi)

Deviator (psi)	Confining (psi)	θ (psi)	τ_{oct} (psi)	2.5%			3.5%			4.5%		
				-10°C	0°C	20°C	-10°C	0°C	20°C	-10°C	0°C	20°C
2.7	3	12	1.2728	1399	1722	410	1695	1530	458	1534	1409	305
5.4	3	15	2.5456	2072	2177	415	2350	2172	454	2428	1817	318
8.1	3	18	3.8184	2559	2387	426	2747	2493	474	2855	1989	332
4.5	5	20	2.1213	2246	2208	428	2399	2094	473	2323	1875	337
9	5	25	4.2426	2828	2451	444	2994	2613	497	3031	2039	342
13.5	5	30	6.3640	2898	2533	435	3268	2880	497	3214	2023	344
9	10	40	4.2426	2908	2422	490	3110	2647	518	3120	2011	361
18	10	50	8.4853	2882	2700	477	3439	3159	537	3405	1720	368
27	10	60	12.7279	2932	2671	470	3424	3157	543	3467	1341	369
9	15	55	4.2426	2692	2553	518	3072	2792	549	3274	1644	394
13.5	15	60	6.3640	2816	2732	517	3201	3075	566	3455	1607	394
27	15	75	12.7279	2978	2757	503	3488	3201	564	3535	1326	390
13.5	20	75	6.3640	2857	2661	552	3200	2969	575	3560	1320	418
18	20	80	8.4853	3051	2727	547	3370	3125	570	3647	1322	412
36	20	100	16.9706	3209	2733	533	3470	3257	586	3573	1337	410

Table 4 M_R of EATB, Northern Region (ksi)

Deviator (psi)	Confining (psi)	θ (psi)	τ_{oct} (psi)	1.5%			2.5%			3.5%		
				-10^oC	0^oC	20^oC	-10^oC	0^oC	20^oC	-10^oC	0^oC	20^oC
2.7	3	12	1.2728	1026	897	367	1152	1880	271	1586	1088	250
5.4	3	15	2.5456	1314	1009	325	1540	2625	185	1866	1079	219
8.1	3	18	3.8184	1378	983	304	1678	2410	182	1991	1141	198
4.5	5	20	2.1213	1439	1118	358	1739	2553	234	1929	1157	311
9	5	25	4.2426	1409	1049	314	1801	2598	199	2054	1139	218
13.5	5	30	6.3640	1417	1101	310	1863	1755	196	2018	1149	216
9	10	40	4.2426	1507	1182	376	1978	1367	233	2214	1192	253
18	10	50	8.4853	1424	1198	354	1926	1226	223	1999	1202	244
27	10	60	12.7279	1411	1217	330	1833	1266	214	1795	1231	240
9	15	55	4.2426	1465	1197	391	1960	1424	257	2372	1298	276
13.5	15	60	6.3640	1458	1207	379	1905	1312	246	2247	1233	268
27	15	75	12.7279	1493	1245	362	1862	1316	233	1884	1247	262
13.5	20	75	6.3640	1452	1266	414	2024	1305	267	2518	1291	286
18	20	80	8.4853	1476	1253	412	1946	1330	265	2181	1285	284
36	20	100	16.9706	1541	1297	374	1882	1363	246	1915	1280	275

Table 5 M$_R$ of EATB, Central Region (ksi)

Deviator (psi)	Confining (psi)	θ (psi)	τ_{oct} (psi)	1.5%			2.5%			3.5%		
				-10°C	0°C	20°C	-10°C	0°C	20°C	-10°C	0°C	20°C
2.7	3	12	1.2728	1299	963	465	2648	868	372	2395	2188	446
5.4	3	15	2.5456	1787	929	518	4325	891	387	3773	2267	437
8.1	3	18	3.8184	2114	987	554	4716	978	406	3085	2086	435
4.5	5	20	2.1213	1806	981	538	3738	1007	410	3846	2494	432
9	5	25	4.2426	2399	984	584	4556	995	428	2602	2120	441
13.5	5	30	6.3640	2548	1048	618	4408	1027	441	2415	1685	437
9	10	40	4.2426	2823	1013	622	4470	1042	479	2698	1394	472
18	10	50	8.4853	2894	1069	669	4264	1085	474	2364	1192	467
27	10	60	12.7279	2834	1064	643	3902	1146	457	2269	1175	452
9	15	55	4.2426	2976	1104	641	4208	1064	511	2724	1145	500
13.5	15	60	6.3640	3329	1137	674	4446	1085	511	2499	1186	504
27	15	75	12.7279	3267	1112	672	3930	1146	495	2242	1180	476
13.5	20	75	6.3640	3145	1110	703	4252	1124	540	2495	1177	535
18	20	80	8.4853	3419	1155	717	4254	1147	537	2369	1225	520
36	20	100	16.9706	3099	1184	698	3947	1195	504	2112	1194	488

88

Table 6 M_R of EATB, Southeast Region (ksi)

Deviator (psi)	Confining (psi)	θ (psi)	τ_{oct} (psi)	1.5%			2.5%			3.5%		
				-10^oC	0^oC	20^oC	-10^oC	0^oC	20^oC	-10^oC	0^oC	20^oC
2.7	3	12	1.2728	1359	1383	446	1479	1252	345	1752	2888	292
5.4	3	15	2.5456	1567	1342	396	1589	991	322	1418	2327	265
8.1	3	18	3.8184	1552	1384	388	1678	857	320	1423	2166	263
4.5	5	20	2.1213	1588	1578	403	1536	876	339	1716	2562	285
9	5	25	4.2426	1662	1370	403	1526	806	334	1460	2221	284
13.5	5	30	6.3640	1655	1363	402	1526	781	330	1361	2120	282
9	10	40	4.2426	1666	1245	433	1511	858	363	1383	2221	313
18	10	50	8.4853	1702	1281	440	1256	832	362	1401	1978	313
27	10	60	12.7279	1648	1327	425	1238	851	344	1386	1525	302
9	15	55	4.2426	1647	1267	468	1251	901	381	1415	2064	332
13.5	15	60	6.3640	1728	1314	467	1206	909	386	1381	1876	346
27	15	75	12.7279	1700	1335	450	1254	910	373	1409	1443	325
13.5	20	75	6.3640	1801	1372	476	1246	945	407	1524	1876	365
18	20	80	8.4853	1793	1395	490	1244	938	414	1518	1579	363
36	20	100	16.9706	1705	1317	459	1288	934	379	1451	1280	340

Table 7 M_R of FATB, Northern Region (ksi)

Deviator (psi)	Confining (psi)	θ (psi)	τ_oct (psi)	1.5%			2.5%			3.5%		
				-10°C	0°C	20°C	-10°C	0°C	20°C	-10°C	0°C	20°C
2.7	3	12	1.2728	143	71	36	210	72	41	72	48	24
5.4	3	15	2.5456	165	78	41	216	79	46	79	53	30
8.1	3	18	3.8184	179	88	49	221	89	53	88	61	38
4.5	5	20	2.1213	157	56	38	211	77	43	75	50	27
9	5	25	4.2426	184	90	50	226	90	55	91	63	39
13.5	5	30	6.3640	210	112	67	244	113	70	111	81	52
9	10	40	4.2426	187	96	53	246	96	59	94	68	40
18	10	50	8.4853	216	132	82	260	130	85	118	95	61
27	10	60	12.7279	208	155	105	230	153	98	121	112	66
9	15	55	4.2426	141	99	60	195	94	68	75	68	34
13.5	15	60	6.3640	156	112	67	204	106	73	85	77	43
27	15	75	12.7279	205	158	106	233	156	101	123	115	71
13.5	20	75	6.3640	153	113	71	209	111	81	87	80	44
18	20	80	8.4853	170	126	80	218	124	88	100	92	67
36	20	100	16.9706	201	169	115	228	171	130	133	128	83

Table 8 M_R of FATB, Central Region (ksi)

Deviator (psi)	Confining (psi)	θ (psi)	τ_{oct} (psi)	1.5%			2.5%			3.5%		
				-10°C	0°C	20°C	-10°C	0°C	20°C	-10°C	0°C	20°C
2.7	3	12	1.2728	224	155	182	234	105	58	125	75	36
5.4	3	15	2.5456	283	174	175	226	117	60	126	75	41
8.1	3	18	3.8184	331	197	173	235	128	67	130	79	50
4.5	5	20	2.1213	331	176	179	248	117	58	131	74	41
9	5	25	4.2426	341	207	175	256	129	69	137	81	53
13.5	5	30	6.3640	373	237	187	262	149	87	152	96	68
9	10	40	4.2426	377	213	190	309	137	73	165	86	65
18	10	50	8.4853	391	256	204	302	160	102	178	111	86
27	10	60	12.7279	383	288	218	290	176	126	174	130	101
9	15	55	4.2426	366	218	194	326	126	73	157	87	66
13.5	15	60	6.3640	357	226	187	336	135	82	158	95	71
27	15	75	12.7279	395	299	220	333	175	126	187	136	104
13.5	20	75	6.3640	370	232	194	380	138	85	174	99	77
18	20	80	8.4853	376	253	196	387	151	97	178	111	85
36	20	100	16.9706	388	323	229	357	197	142	202	155	117

Table 9 M_R of FATB, Southeast Region (ksi)

Deviator	Confining	θ	τ_{oct}	1.5%			2.5%			3.5%		
(psi)	(psi)	(psi)	(psi)	-10°C	0°C	20°C	-10°C	0°C	20°C	-10°C	0°C	20°C
2.7	3	12	1.2728	347	431	139	354	208	162	257	178	81
5.4	3	15	2.5456	350	289	126	386	271	159	269	212	79
8.1	3	18	3.8184	349	263	127	387	289	166	282	220	84
4.5	5	20	2.1213	353	434	133	379	277	163	264	199	80
9	5	25	4.2426	353	301	128	392	300	166	283	219	85
13.5	5	30	6.3640	354	283	140	400	321	182	303	235	98
9	10	40	4.2426	350	283	133	397	315	183	287	232	89
18	10	50	8.4853	341	273	155	408	347	198	301	255	110
27	10	60	12.7279	313	290	172	383	370	211	292	275	122
9	15	55	4.2426	279	312	138	358	330	180	249	238	88
13.5	15	60	6.3640	280	274	139	361	329	178	253	237	91
27	15	75	12.7279	309	293	170	384	372	210	293	278	120
13.5	20	75	6.3640	275	276	140	362	342	181	258	242	93
18	20	80	8.4853	288	273	146	369	342	183	269	247	100
36	20	100	16.9706	321	307	179	383	379	213	294	286	130

Table 10 M_R of 50:50 RAP (ksi)

Deviator (psi)	Confining (psi)	θ (psi)	τ_{oct} (psi)	Northern			Central			Southeast		
				-10°C	-2°C	20°C	-10°C	-2°C	20°C	-10°C	-2°C	20°C
2.7	3	12	1.2728	643	638	16	952	1073	15	2462	668	17
5.4	3	15	2.5456	556	617	17	879	895	17	3941	609	19
8.1	3	18	3.8184	572	640	20	844	899	19	4095	643	21
4.5	5	20	2.1213	560	841	22	1176	1012	22	3745	712	24
9	5	25	4.2426	581	791	25	858	919	25	3853	633	26
13.5	5	30	6.3640	584	791	27	950	978	27	3760	625	28
9	10	40	4.2426	602	915	36	1230	1043	36	3639	667	37
18	10	50	8.4853	614	844	38	1181	974	38	2740	635	40
27	10	60	12.7279	622	862	40	1116	959	39	2289	613	42
9	15	55	4.2426	610	977	42	1308	1135	43	3269	935	45
13.5	15	60	6.3640	630	885	43	1353	1065	44	2755	925	46
27	15	75	12.7279	652	885	48	1268	1005	47	2113	831	50
13.5	20	75	6.3640	727	919	51	1393	1164	51	2194	1119	54
18	20	80	8.4853	813	931	53	1379	1090	52	2093	1072	55
36	20	100	16.9706	888	906	58	1371	1036	57	1990	959	61

93